Institutionen för vattenbyggnad
Chalmers tekniska högskola

Department of Hydraulics
Chalmers University of Technology

BEDLOAD TRANSPORT IN STORM SEWERS
Stream Traction in Pipe Channels

by

Gustavo S. Perrusquía González

Submitted to the School of Civil Engineering, Chalmers University of Technology in partial fulfillment of the requirements for the degree of Doctor of Philosophy.

Opponent: Emeritus Professor P. Novak, Newcastle upon Tyne, England

Report
Series A:22
ISSN 0348-1050

Göteborg 1991

Address: Department of Hydraulics
Chalmers University of Technology
S-412 96 Göteborg, Sweden

Telephone: 031-72 10 00

"There are no exhausted topics, only exhausted men in the topics"

Professor Abraham Díaz, National University, Mexico City, 1980.

ABSTRACT

The hydraulics of sediment transport in part-full pipes was investigated in an experimental study. The sediment bed was permanently deposited and the type of transport observed and measured was bedload transport exclusively. The experiments were performed in a concrete pipe, 225 mm in diameter and 23 m long. Two sand sizes, D_{50} = 0.9 mm and 2.5 mm, were used. Two sediment bed thicknesses were tested, namely 0.2 D and 0.4 D (D being the pipe diameter). Pipe slopes ranged from 0.002 to 0.006.

Two complementary series of experiments were conducted at Hydraulics Research Ltd. in Wallingford and at The University of Newcastle upon Tyne, both in England. Different pipe diameters, sediment sizes and sediment bed thicknesses were tested. This additional information allowed the present study a wider range of application.

Three procedures, commonly used in this kind of experimental study, were tested to corroborate the validity of the proposed methods: 1) the vertical velocity distribution near the sediment bed can be described by a logarithmic law referred to as the velocity-defect law, 2) the side wall elimination procedures of Einstein and Vanoni-Brooks can be used to compute the hydraulic radius of the sediment bed with an accuracy which is acceptable for engineering purposes, and 3) the critical shear stress of the sediment particles can be obtained by using Shields' diagram with good approximation.

The methods of Engelund-Hansen and van Rijn for the prediction of flow resistance in alluvial channels were used to compare their predicted values with the experimental data. Both methods gave approximate agreements. A procedure which can be used as a design method for the conditions of the present study was proposed.

Bedform dimensions (height and length) were also measured and compared with the predictors given by the methods of Fredsøe and van Rijn for the prediction of bedform geometry in alluvial channels. The agreement was poor and the methods have to be modified for pipe-channel conditions.

A relationship to estimate sediment transport rates, based on dimensional analysis, was proposed. This relationship is expressed in terms of both flow and particle parameters as well as geometric (shape) factors. The range of application for pipe diameter (D) is 154 mm to 225 mm, for sand size (D_{50}) is 0.5 mm to 2.5 mm, for pipe slope (S) is up to 0.006 and for sediment thickness (t) is up to 0.4 D.

Five available equations for bedload transport computation were used for comparison with the proposed relationship. The equations of Novak & Nalluri and Einstein & Brown, in which transport is exclusively a function of shear stress, gave better estimates than the equations of Meyer-Peter & Müller, Engelund & Fredsøe and van Rijn, which are based on the excess shear.

Both the procedure for the prediction of flow resistance and the proposed relationship for bedload transport estimation can be used in the analysis of storm sewer systems. Further experimental work with larger pipe diameters, mixed gradings, different levels of sediment and unsteady flow conditions is needed before these methodologies can be fully incorporated in a simulation model for sediment transport in sewers.

PREFACE

In 1985 the Department of Hydraulics, Chalmers University of Technology, initiated research on "Sedimentation and Erosion in Sewers". The project was included within the framework of research for the Urban Geohydrology Research Group. Financial support was provided by the Swedish Council for Building Research. Prior to this report, the following publications have been produced:

1) Perrusquía, G., Lyngfelt, S., and Sjöberg, A. (1986): Capacity of sewers partly filled with sediment. A preliminary theoretical and experimental study. Chalmers University of Technology, Department of Hydraulics, Report Series B:48, Göteborg, Sweden. (In Swedish).

2) Perrusquía, G., Lyngfelt, S., and Sjöberg, A. (1987): Flow capacity of sewers with a sediment bed. Proceedings 4th IAHR International Conference on Urban Storm Drainage, Lausanne, Switzerland.

3) Perrusquía, G. (1988): Part-full flow in pipes with a sediment bed. Part one: Bedform dimensions. Part two: Flow resistance. Chalmers University of Technology, Department of Hydraulics, Report Series A:17, Göteborg, Sweden. (Thesis presented in partial fulfillment of the requirements for the degree of Licentiate of Engineering).

4) Perrusquía, G. (1990): Flow resistance in storm sewers with a sediment bed. Proceedings 5th IAHR International Conference on Urban Storm Drainage, Osaka, Japan.

5) Perrusquía, G. (1990): Sediment in sewers. Research leaves. Part one: Wallingford, October-November 1989. Part two: Newcastle, March-April 1990. Chalmers University of Technology, Department of Hydraulics, Report Series B:52, Göteborg, Sweden.

This independent thesis is submitted by the author in partial fulfillment of the requirements for the degree of Doctor of Philosophy in Hydraulic Engineering. However, the methodologies and results from the previous reports are referred to herein because they are part of the investigation.

Göteborg, October 1991 Gustavo S. Perrusquía G.

ACKNOWLEDGEMENTS

My first contact with Chalmers was in 1980 while on vacation. I talked to Professor Anders Sjöberg about the possibility of undertaking doctoral studies at the Department of Hydraulics. In 1984 I came to Chalmers to spend my sabbatical leave from the University of Querétaro in Mexico. A year later I got a position as research assistant to study the transport of non-cohesive particles in storm sewers. Ever since the very first meeting Professor Sjöberg, my advisor, has provided me with constant support and guidance. He believed in me and I am most grateful to him.

I also want to thank Dr. Sven Lyngfelt, co-ordinator of the project, who encouraged me through all stages of my experimental studies. I was lucky to have the assistance of the best team anybody can wish for in the laboratory. No measurements had been accomplished without the help of Mr. Bengt Carlsson and his instrumental inventions, Mr. Karl-Oskar Djärv and his artistic constructions, and Mr. Lars-Ove Sörman in preparing the equipment. Ms. Ann-Marie Holmdahl helped me edit part of the manuscript and Dr. Greg Morrison corrected the language. Comments on the text by Mr. Ole Mark from the University of Aalborg, Denmark were very useful.

I have enjoyed having many interesting discussions with the staff of the department, especially Dr. Lars Bergdahl, Dr. Steffen Häggström and Mr. Gösta Lindvall. The latter also made the necessary arrangements in the laboratory so that instruments and materials were readily available.

The project was funded by the Swedish Council for Building Research (BRF). Mr. Örjan Eriksson and Mr. Jan Falk are gratefully acknowledged. I had the opportunity to travel all over the world representing Chalmers University of Technology. The financial support was provided by the Swedish Council for Building Research and further by contributions from the Royal Swedish Academy of Engineering Sciences, the Åke and Greta Lisshed Foundation, the Adlerbertska Fund and the Chalmers Research Fund.

Last but not least, I want to dedicate this work to Monica, my wife, for her understanding especially during the long absences I had to take in the name of science.

TABLE OF CONTENTS

LIST OF FIGURES

LIST OF TABLES

NOTATION

A	hydraulic area
B	roughness function
C_v	volumetric concentration of sediment
C'	Chezy's grain roughness coefficient
D	pipe diameter
D_{50}	particle diameter of bed material 50% being finer
D_{90}	particle diameter of bed material 90% being finer
D_*	particle number
f	Darcy-Weisbach's friction factor
f_b	Darcy-Weisbach's friction factor of the bed
f_w	Darcy-Weisbach's friction factor of the wall
g	acceleration due to gravity
H	bedform height
k_b	equivalent bedform roughness
k_b'	equivalent grain roughness
k_b''	equivalent bedform roughness
k_r	relative pipe roughness
k_s	equivalent sand roughness
k_w	equivalent wall roughness
L	bedform length
n	Manning's roughness coefficient
n_b	Manning's bed roughness coefficient
n_w	Manning's wall roughness coefficient
P_b	bed wetted perimeter
P_w	wall wetted perimeter
Q	water discharge
Q_b	sediment transport rate
q_b	sediment transport rate per unit width
R	mean hydraulic radius
R_b	hydraulic radius of the bed
R_w	hydraulic radius of the walls
Re_*	grain Reynolds number
S	pipe slope/energy gradient
S'	grain energy gradient
S''	bedform energy gradient
s	relative density of the sediment
T	transport stage parameter

t	sediment bed thickness
t_r	relative bed thickness
u	local flow velocity
u_{max}	maximum local flow velocity
u_*	shear velocity
u_*'	grain shear velocity
u_{*_c}	Shields' critical shear velocity
V	mean flow velocity
V_b	mean flow velocity appropriate to the bed
V_c	critical velocity for the incipient motion of particles in flume traction
V_m	minimum flow velocity for a deposit bed of 1/100 of the pipe diameter
V_s	self-cleansing velocity
V_w	mean flow velocity appropriate to the walls
Y	flow depth
Y_r	relative flow depth
Y'	boundary layer thickness of the bed material transported as bedload
y	height above the sediment bed
y_{max}	height at which the maximum local flow velocity occurs
Z	relative grain size
β	dynamic friction coefficient
Θ_b	dimensionless bed shear stress (bed mobility number)
Θ_b'	dimensionless grain shear stress (grain mobility number)
Θ_b''	dimensionless bedform shear stress
Θ_c	critical dimensionless bed shear stress (critical mobility number)
μ	dynamic viscosity
ν	kinematic viscosity
ρ	density of water
ρ_s	density of sediment
τ_b	bed shear stress
τ_b''	bedform shear stress
Φ_b	transport parameter
Ψ_b	flow intensity parameter

1 INTRODUCTION

1.1 Background, presentation of the problem and scope of the study

Background. The motion of sediment particles in water has been studied by many researchers. However, it was not until the 1930's that the concept "sediment transport" started to be used in scientific circles. The problem that fascinated researchers most was the incredible amount of solid minerals, from rocks to clay, that the world's large rivers carried and deposited long distances downstream. Soon this was the subject of mathematical theories and laboratory-based models. The information that came out of these studies resulted in books and manuals on sediment transport in alluvial rivers.

In recent years, attention has focussed on studying the complicated storm sewer systems that cities have developed. The problems in such systems are similar to those present in surface river systems. The main difference is that storm sewers are man-made and a major problem is to design the system in such a way that both water and sediment are transported satisfactorily. In the mid 1970's and early 1980's several experimental studies, intended to solve the problem of deposition and accumulation of sediment in sewers, were undertaken around the world. Various methods were suggested for the design of self-cleansing sewers.

Presentation of the problem. The accumulation of sediment in storm sewers is still a major problem. Low flows accompanied by mild hydraulic gradients cause deposition. This situation deteriorates until more or less permanent sediment beds build up along the pipe's invert. Depending on the flow conditions the sediment bed may be either plane or with associated bedforms. At the same time, the flow conditions are closely related to the bed resistance which in turn depends on the type of bedforms.

The problem is then the interaction of the flow and the alluvial bed. This situation, which is here named **bedload transport in storm sewers**, particularly **stream traction in pipe channels**, has not been sufficiently investigated in the past and the state of knowledge is rather vague despite the vast amount of information on alluvial channels and sewers. Regarding the latter, previous studies have mainly covered the initiation of motion of sediment particles both in part-full and full pipes and with or without (flume traction) deposited sediment beds.

The hydraulic section of a part-full pipe with a sediment bed is that of a modified (truncated) circular open channel which may produce certain shape effects. Also, alluvial channels are often considered to be wide with no side-wall influence. In contrast, pipes with sediment often have small channel width/flow depth ratios and the side walls may affect the flow process.

Therefore, there is a need for more information to answer the above mentioned uncertainties regarding pipes carrying a significant bedload.

Scope of the study. In two earlier studies, the author investigated: 1) flow resistance in part-full pipes with plane sediment beds with and without transport, and 2) flow resistance and bedform dimensions in pipes with movable sediment beds. However, sediment transport rates were not measured at that stage and flow resistance could not be verified other than by using the available methods applicable to alluvial channels. The present study reports a series of experiments in which all three parameters, i.e. flow resistance, bedform dimensions and sediment transport rate have been measured.

An experimental study of the transport of sediment in a part-full sewer, or pipe channel, was carried out at the Department of Hydraulics, Chalmers University of Technology, Göteborg, Sweden. Experiments were confined to bed load, or stream traction, transport. Uniform sediment sizes were used. The sediment bed was either plane where sediment was stationary or transported or with bedforms where sediment was transported. Fig. 1.1 shows an illustration for the case of movable bedforms.

The purpose of this thesis is to analyze the flow conditions that characterize the stream traction in pipe channels and their relationship to sediment transport rate, flow resistance and bedform dimensions based on previous and present experiments made by the author and on relationships suggested by other authors. Further, the assumptions of a logarithmic velocity distribution, the side wall elimination procedure, and the critical shear stress as obtained from Shields' diagram, all commonly used (but seldom verified) in this type of experimental study, were all tested to corroborate the validity of the computations.

To the author's knowledge this is the first attempt to study the sediment transport in a part-full pipe with a permanently deposited alluvial bed. This experimental study was designed to simulate field conditions as closely as possible since the pipe material was concrete and the sediments were real size particles similar to

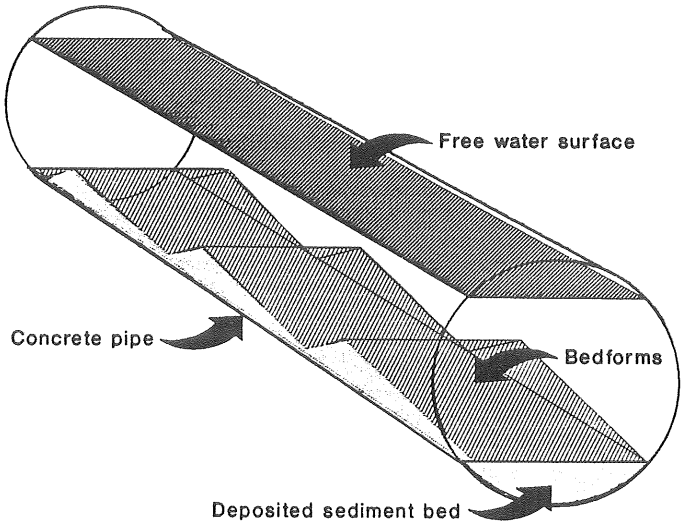

Fig 1.1 Illustration of stream traction in pipe channels

those found in the field. Two complementary series of experiments were carried out by the author at the Department of River Engineering, Hydraulics Research Ltd. and at the Hydraulics Laboratory of the Department of Civil Engineering, The University of Newcastle upon Tyne, both in England. Different pipe diameters were used to cover a wider range of pipe dimensions. The results from these experiments are also reported in this thesis.

In Chapter 2, basic concepts in hydraulics of stream traction as well as a review of studies by other researchers and by the author are described. A dimensional analysis for the case of stream traction in pipe channels and the functional relationship for the phenomenon are presented in Chapter 3.

Chapter 4 describes the apparatus, the instruments used and the experimental procedure, while Chapter 5 presents an analysis of the results. A brief summary with conclusions and recommendations for further work are presented in Chapter 6.

2 PART-FULL PIPES WITH A DEPOSITED SEDIMENT BED

2.1 Definitions

Sediment transport in pipe channels was briefly described in the previous chapter. However, a better definition of the phenomenon is required in order to clarify the flow conditions this study assumes and therefore a brief list of definitions is presented below:

Bedforms. The irregularities that form on the surface of the sediment bed. The most common forms for the present hydraulic conditions are ripples and dunes.

Bedload transport. The mode of sediment transport in which the particles move in close contact with the sediment bed. These particles move either by sliding, rolling or jumping.

Pipe-channel flow. Free surface flow in a circular section. In the present study, the circular section is truncated due to the presence of the sediment bed. An additional concept is intrinsic to this type of flow: Narrow channels, due to the limited width of the section. The side-wall effect can no longer be disregarded.

Side-wall elimination procedure. A method that separates the influence of the side walls from that of the sediment bed. This is particularly useful when the hydraulic characteristics corresponding to the sediment bed are being computed.

Stationary flow. The state of motion achieved when the mass flow is constant. Both fluid and sediment transport must be in equilibrium.

Stream traction. The transport of particles as bedload on a deposited sediment bed. This is the case when dealing with alluvial channels. Stream traction differs from flume traction in that the latter occurs on the invert of the pipe, i.e. there is no deposited bed.

2.2 Flow Characteristics

The aim of this section is to describe three main assumptions that are commonly used in this kind of experimental study, namely the logarithmic velocity distribution, the side wall elimination and the critical shear stress. The procedures to obtain the logarithmic velocity profiles, the hydraulic radius corresponding to the sediment bed and the critical shear stress are also presented in this section. The validity of the three assumptions and the results are covered in Chapter 5.

2.2.1 Velocity distribution

To determine flow resistance on sediment beds, knowledge of the shear stress over the boundary is required. Shear stress can in turn be defined by assuming that the velocity distribution follows a logarithmic law commonly referred to as the law of the wall. The representation of the law of the wall varies depending on whether the flow regime is hydraulically smooth, transitional or rough. A dimensionless parameter that provides a criterion to identify the type of flow is the grain Reynolds number

$$Re_* = \frac{u_* \, D_{50}}{\nu} \qquad (2.1)$$

in which $u_* = \sqrt{\tau_b/\rho}$ = shear velocity; τ_b = shear stress; ρ = density of water; D_{50} = particle diameter of bed material 50% being finer; and ν = kinematic viscosity of water.

Bedforms are said to be related to the type of flow; ripples occur if the flow is hydraulically smooth, dunes occur if the flow is hydraulically rough (Allen 1968, Engelund and Fredsøe 1982, van Rijn 1984B). In the experiments reported in this thesis, bedforms were identified in both the transitional and hydraulically rough flow regimes, i.e. in both the transitional region from ripples to dunes and in the region where dunes definitely occur. The ranges of Re_* for both flow regimes are:

$$5 < Re_* < 70 \qquad \text{transitional} \qquad (2.2)$$

$$Re_* > 70 \qquad \text{rough} \qquad (2.3)$$

Eqs. (2.2) and (2.3) are suitable for wide open channels. However, these equations can be applied to pipe channels, considering the latter to be analogous to open channels, since only the hydraulic properties of the sediment bed are considered. The equation used in the present study for the average velocity in a vertical profile is that attributed to Einstein (Graf 1984, Lau 1988, Simons and Şentürk 1977) and Keulegan (Chow 1959, Raudkivi 1976, Whiting and Dietrich 1990):

$$\frac{V}{u_*} = 5.75 \log\left[10^{(B/5.75)} \left[\frac{R_b}{2.5\ k_b}\right]\right] \qquad \text{transitional} \qquad (2.4)$$

$$\frac{V}{u_*} = 5.75 \log\left[12 \frac{R_b}{k_b}\right] \qquad \text{rough} \qquad (2.5)$$

in which V = mean flow velocity; B = roughness function in terms of Re_* which has a value of 8.5 for hydraulically rough flow ($Re_* > 70$); R_b = hydraulic radius corresponding to the sediment bed; and k_b = equivalent sand roughness of the bed. The value of B can be obtained from Nikuradse's roughness curve as given by Simons and Şentürk (1977).

In the present study, the assumption that the velocity distribution follows a logarithmic law has been tested and found valid. Vertical velocity profiles were measured at the centerline and compared with the corresponding velocity-defect relationship which can generally be expressed as

$$\frac{u_{max}-u}{u_*} = 5.75 \log\left[\frac{y_{max}}{y}\right] \qquad (2.6)$$

in which u = local flow velocity at a height y above the sediment bed.

The agreement was found to be satisfactory which means that a logarithmic velocity distribution can be assumed near the sediment bed.

2.2.2 Side wall elimination

The boundaries of the cross sections investigated in the present study are the side walls of the pipe and the sediment bed. The cross sections cannot be regarded as wide as is often the case for alluvial channels. Therefore, the properties of the sediment bed should be computed separately from those of the side walls. A common technique used for the estimation of the parameters that are exclusively related to the sediment bed is the **side-wall elimination procedure.**

The procedures used in the present study to determine the hydraulic radius of the sediment bed were those suggested by Einstein (1942) and Vanoni-Brooks (1957). The former uses Manning's equation while the latter uses Darcy Weisbach's equation, both described in detail in Perrusquía et al (1986). These elimination procedures are based on the assumption that the cross section can be divided into two subsections; one related to the sediment bed and the other to the side walls. Each of these subsections are assumed to have the same average velocity and hydraulic gradient. The procedures lead to Eqs. (2.7) to (2.10) which are outlined below:

2.2.2.1 Computational procedures using Manning's equation

The hydraulic radius of the bed, R_b, can be computed using the side wall elimination procedure of Einstein (1942):

$$A = R_w P_w + R_b P_b \tag{2.7}$$

and Manning's equation applied to both side walls and sediment bed

$$V = \frac{1}{n_w} R_w^{\frac{2}{3}} S^{\frac{1}{2}} \qquad \text{side wall}$$

$$V = \frac{1}{n_b} R_b^{\frac{2}{3}} S^{\frac{1}{2}} \qquad \text{sediment bed} \tag{2.8}$$

in which A = total hydraulic area; n = Manning's roughness coefficient; P = wetted perimeter; R = hydraulic radius; S = energy slope; and subscripts w and b denote wall and bed components respectively.

Substitution of Eq. (2.8) which is appropriate to the walls (i.e. knowing n_w and P_w) into Eq. (2.7) gives R_b (knowing P_b) from which the Manning's roughness coefficient of the bed, n_b, can be computed using Eq. (2.8) appropriate to the bed.

2.2.2.2 Computational procedures using Darcy-Weisbach's equation

The friction factor, f, for the bed or walls is computed using the Colebrook-White equation

$$f^{-\frac{1}{2}} = -2 \log \left[\frac{k_s}{14.8\ R} + \frac{2.51\ \nu}{R\sqrt{128\ g\ R\ S}} \right] \tag{2.9}$$

in which g = acceleration due to gravity; and k_s = equivalent sand roughness.

This assumes that Eq. (2.9) can be applied to all the subsections (side walls and sediment bed) of the part-full pipe flow. The assumption $V_w = V_b$ (=V) combined with Darcy-Weisbach's equation (Vanoni-Brooks 1957) also gives:

$$\frac{f_w}{R_w} = \frac{f_b}{R_b} \tag{2.10}$$

Combining Eqs. (2.7), (2.9) and (2.10) gives R_w and R_b (this is done iteratively and generating values for the equivalent sand roughness of both bed and walls, k_b and k_w respectively). f_w and f_b can then be computed using Eq. (2.9). In solving these equations, pipe diameter, D, flow depth, Y, sediment bed thickness, t, and energy slope, S, are known.

In this study, the assumption that the side-wall elimination procedure can be applied even to narrow channels has been tested and found valid. The value of shear velocity, u_*, was identified as the slope of the line produced by the logarithmic velocity distribution according to Eq. (2.6). Bed shear stresses were computed from the expression: $\tau_b = u_*^2 \rho$. The hydraulic radius of the bed, R_b, was then determined from the bed shear stress using the expression

$$\tau_b = \rho g R_b S \qquad (2.11)$$

This experimental value of R_b was finally compared with that from the elimination procedure and fairly good agreement between these two values was found in most cases.

2.2.3 Critical shear stress

The initiation of motion has been widely studied and the critical shear stress has been incorporated in various transport parameters which are expressed in terms of an excess shear stress. This concept represents the minimum flow resistance exerted by the particles at the moment before the initiation of motion. In the present study, the critical shear stress was determined using the experimental data. The rate of sediment transport in volume per unit time, Q_b, was measured and plotted against its corresponding bed shear stress, τ_b. Both Q_b and τ_b are dimensional parameters and it is convenient to express them as their respective dimensionless counterparts. Thus, Q_b can be replaced by the volumetric concentration

$$C_v = \frac{Q_b}{Q} \times 10^6 \qquad (2.12)$$

in which C_v = volumetric concentration in parts per million; Q = water discharge (the rate of fluid transport in volume per unit time). τ_b can in turn be replaced by the dimensionless bed shear stress

$$\Theta_b = \frac{\tau_b/\rho}{g(s-1)D_{50}} = \frac{R_b S}{(s-1)D_{50}} \qquad (2.13)$$

in which Θ_b = dimensionless bed shear stress; and $s = \rho_s / \rho$ = relative density of the sediment; ρ_s being the density of sediment.

The volumetric concentration, C_v, can be plotted against the dimensionless bed shear stress, Θ_b, to find the critical value for the dimensionless bed shear stress, Θ_c, where the value of C_v is 1 ppm. Critical shear stresses were found to be in the vicinity of Shields' curve.

2.3 Review of related work for the present study

The majority of studies on sediment transport have been done in alluvial channels. The studies in sewers have mainly dealt with incipient motion problems in flume traction. However, the hydraulic principles upon which they are based can still be applied to the case of part-full pipes with a sediment bed subject to stream traction. The three basic concepts treated in this thesis are flow resistance, bedform dimensions and sediment transport rate. They are discussed here together with those studies closely related to the present investigation.

2.3.1 Flow resistance

As soon as bedforms appear on the bed surface, flow resistance is assumed to be made up of two main components: one depending on **grain resistance** and the other on **form resistance**. In the present study, flow resistance will be referred exclusively to the sediment bed. Flow resistance can be calculated by a variety of parameters such as the dimensionless bed shear stress, Θ_b, and the equivalent sand roughness of the bed, k_b. Both approaches are briefly outlined below using two different methods to predict flow resistance in alluvial channels.

2.3.1.1 Engelund-Hansen's method for the determination of bed shear stress

The dimensionless bed shear stress can be expressed as

$$\Theta_b = \Theta_b' + \Theta_b'' \qquad (2.14)$$

in which Θ_b' and Θ_b'' are the dimensionless shear stresses of the grain and bedforms respectively.

The dimensionless grain shear stress Θ_b' is defined as

$$\Theta_b' = \frac{(u_*')^2}{(s-1)g\,D_{50}} \tag{2.15}$$

in which u_*' = grain shear velocity.

The grain shear velocity can be calculated from Eq. (2.16) which is similar to that of Einstein:

$$\frac{V}{u_*'} = 5.75 \log \left[11 \frac{Y'}{k_b'}\right] \tag{2.16}$$

in which k_b' = equivalent grain roughness and Y' = boundary layer thickness which has been defined by Engelund-Hansen (1972), who found this thickness to be fairly constant as shown in Fig. 2.1.

Engelund and Hansen used similarity principles between the sediment layer and the total flow and proposed:

$$\frac{\Theta_b'}{Y'} = \frac{\Theta_b}{Y} \tag{2.17}$$

in which Y = flow depth.

They also suggested a value of $k_b' = 2.5\ D_{50}$. The value of Θ_b' is found iteratively using Eqs. (2.15), (2.16) and (2.17).

The dimensionless shear stress due to bedforms, Θ_b'', is defined as

$$\Theta_b'' = \frac{\tau_b''/\rho}{(s-1)g\,D_{50}} \tag{2.18}$$

in which τ_b'' = bedform shear stress.

Engelund (1966) has proposed that the total energy gradient, S, consists of two components given by

$$S = S' + S'' \tag{2.19}$$

in which the superscripts ' and " relate to grain and bedform respectively.

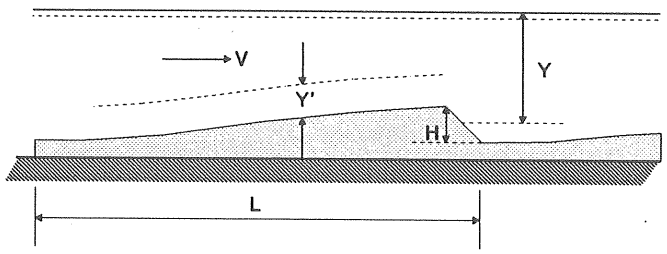

Fig. 2.1 Sketch of bedforms

Engelund and Hansen compared the resistance exerted by the bedforms to the energy dissipated due to the flow expansions after each bedform crest and estimated the bedform energy gradient using Carnot's formula for expansion losses as

$$S'' = \frac{V^2}{2g\ L}\left[\frac{H}{Y}\right]^2 \qquad (2.20)$$

in which H and L are bedform height and length respectively.

Bedform shear stress τ_b'' is written as

$$\tau_b'' = \rho\ g\ Y\ S'' \qquad (2.21)$$

and insertion of Eqs. (2.20) and (2.21) into Eq. (2.18) gives

$$\Theta_b'' = \frac{V^2}{(s\text{-}1)2g\ D_{50}}\left[\frac{H^2}{LY}\right] \qquad (2.22)$$

2.3.1.2 van Rijn's method for the prediction of effective hydraulic roughness

In this method, the equivalent sand roughness of the bed is expressed as

$$k_b = k_b' + k_b'' \tag{2.23}$$

in which the superscripts ' and " also relate to grain and bedform respectively.

van Rijn (1982) computed the equivalent grain roughness, k_b', using the resistance equation in the form

$$\frac{V}{u_{*r}} = 2.5 \ln \left[\frac{R_b}{k_b'} \right] + 6.23 \tag{2.24}$$

This relationship is valid for hydraulically rough flow. For transitional flow, the following relationship was applied:

$$\frac{V}{u_{*r}} = 2.5 \ln \left[\frac{R_b}{k_b' + \frac{3.3\nu}{u_{*r}}} \right] + 6.23 \tag{2.25}$$

van Rijn (1982) analyzed 120 sets of data with plane bed conditions and a channel width/water depth ratio larger than five where no side wall elimination is necessary. He then related k_b' to the particle size D_{90} of the bed material. The suggested relationship for fine to medium sized particles was

$$k_b' = 3\, D_{90} \tag{2.26}$$

The equivalent bedform roughness, k_b'' was found as a function of the bedform height, H and the bedform steepness, H/L. 40 sets of data were used with a channel width/water depth ratio larger than five and a water depth/bedform roughness ratio larger than ten. The resulting best-fitting relationship (for the range $0.01 \leq H/L \leq 0.2$) was given as

$$k_b'' = 1.1\, H \left[1 - e^{(-25\, H/L)} \right] \tag{2.27}$$

2.3.2 Bedform dimensions

The available methods for the estimation of the geometry of the bedforms provide a distinction between ripples and dunes. However, the author prefers to call them

bedforms because in spite of the many different available criteria for the classifi cation of bedforms, the distinction is still a matter open for discussion (Gyr 1989).

2.3.2.1 Fredsøe's method for the calculation of bedform dimensions

This method is based on the assumption that bedform dimensions are related to the bedload transport. To compute the shape of bedforms, Fredsøe (1982) used the bed shear stress distribution downstream a dune-like step. Bedform height, H, was related to the flow depth, Y, and a dimensionless transport parameter, Φ_b. Bedform length, L, was expressed in a differential equation that gives the variation in height with length and an approximation to that equation was given by the Danish Hydraulic Institute (1986). Fredsøe's method is related to some extent to the theories proposed by Engelund and Hansen (Fredsøe 1974, 1979). For a complete description of this method, see Perrusquía (1988).

Fredsøe used the Meyer-Peter & Müller formula

$$\Phi_b = 8(\Theta_b' - \Theta_c)^{\frac{3}{2}} \qquad (2.28)$$

in which Φ_b = dimensionless transport parameter, and the following relation for bedform height to flow depth was produced:

$$\frac{\frac{H}{Y}}{1 - \frac{H}{2Y}} = \frac{\Theta_b' - \Theta_c}{3\Theta_b'} \qquad (2.29)$$

while the relationship for bedform height to length is:

$$\frac{H}{L} = 0.06 - 146\,(0.15 + \Theta_c - \Theta_b)^{4.26} \qquad (2.30)$$

in which Θ_c is Shields' critical dimensionless bed shear stress.

2.3.2.2 van Rijn's method for the prediction of bedform dimensions

This method is also based on the assumption that bedform dimensions are related to bedload transport. van Rijn (1984) analyzed 84 flume and field data considering

only dune-type bedforms. Bedform height, H, was related to the particle diameter, D_{50}, the flow depth, Y, and a transport stage parameter, T; whereas bedform length, L, was found to be exclusively related to the flow depth, Y, as given by:

$$\frac{H}{Y} = 0.11 \left[\frac{D_{50}}{Y}\right]^{0.3} \left[1 - e^{(-0.5\ T)}\right] (25 - T) \qquad (2.31)$$

and

$$L = 7.3\ Y \qquad (2.32)$$

where T = transport stage parameter represented as

$$T = \frac{(u_*')^2 - (u_{*_c})^2}{(u_{*_c})^2} = \frac{\Theta_b' - \Theta_c}{\Theta_c} \qquad (2.33)$$

in which ; u_*' = grain shear velocity expressed as: $(V/C')\sqrt{g}$; C' being Chezy's grain roughness coefficient = 18 log (12 R_b / k_b'); k_b' corresponding to an equival lent bed sand roughness of 3 D_{90}; and u_{*_c} = Shields' critical shear velocity.

2.3.3 Sediment transport

Even though the majority of experimental studies on sediment transport in sewers deal with incipient motion problems in flume traction, i.e. there is no deposited bed, the hydraulic principles upon which they are based can still be applied to the present case.

2.3.3.1 Novak and Nalluri's studies on the initiation of sediment motion over fixed beds

In their first study, Novak and Nalluri (1972) proposed, from Shields' functional relationship and hydraulic principles, an equation for the critical velocity, V_c, for the incipient motion of particles in wide channels

$$\frac{V_c}{\sqrt{g\ D_{50}}} = 1.92\ \sqrt{s-1} \left[\frac{D_{50}}{Y}\right]^{-\frac{1}{6}} \qquad (2.34)$$

Their second study was an experimental analysis in smooth fixed boundary channels with no sediment bed, i.e. flume traction. Novak and Nalluri (1975)

incorporated the relative roughness into the analysis to account for shape effects of the channel. A best-fit relationship in the range $0.01 < D_{50}/R < 1$ was given by

$$\frac{V_c}{\sqrt{g\ D_{50}}} = 0.61\ \sqrt{s\text{-}1}\left[\frac{D_{50}}{R}\right]^{-0.27} \qquad (2.35)$$

in which R = hydraulic mean radius of the channel.

Novak and Nalluri (1975) also suggested a relationship for bedload transport based on their experimental data:

$$\Phi = 11.6\ \Psi^{-2.04} \qquad (2.36)$$

in which the transport parameter, $\Phi = C_v\ VR/\sqrt{g\ (s\text{-}1)(D_{50})^3}$; and the flow intensity parameter, $\Psi = (s\text{-}1)D_{50}/RS$. Here, C_v is expressed as a fraction and not in ppm.

It should be pointed out that the area occupied by the transported sediment is assumed to be negligible. Similar relationships to that expressed in Eq. (2.36) have been presented earlier by Meyer-Peter and Müller (1948), Einstein and Brown (Brown 1950) and Graf (1984), among others (Vanoni 1975). They are, however, designed for wide alluvial channels.

In their third study, also experimental, Novak and Nalluri (1984) proposed a general equation that covers both smooth and rough fixed beds in the form

$$\frac{V_c}{\sqrt{g\ (s\text{-}1)D_{50}}} = a\left[\frac{D_{50}}{R}\right]^b \qquad (2.37)$$

2.3.3.2 May's studies on self-cleansing sewers

Two comprehensive theoretical and experimental analyses on flume traction in sewers were carried out by May (1982, 1989). By fitting his experimental data to a semi-theoretical relationship May (1982) proposed an equation for the limit of deposition

$$C_v = 0.02\left[\frac{D^2}{A}\right]\left[\frac{D_{50}}{R}\right]^{\frac{3}{5}}\left[\frac{V_s^2}{\sqrt{g(s\text{-}1)\ D_{50}}}\right]^{\frac{3}{2}}\left[1\text{-}\frac{V_c}{V_s}\right]^4 \qquad (2.38)$$

in which C_v = volumetric sediment concentration expressed as fraction; V_s = self-cleansing velocity; and V_c is as defined in Eq. (2.35).

In an extension of the previous study, May et al (1989) took into account the proportional depth of flow. This resulted in a simple envelope curve, covering previous and new experimental data, for a deposited sediment bed of t/D = 1% (t being the sediment bed thickness)

$$C_v = 0.04 \left[\frac{D^2}{A}\right] \left[\frac{D_{50}}{R}\right]^{\frac{3}{5}} \left[\frac{Y}{D}\right]^{0.36} \left[\frac{V_m^2}{\sqrt{g(s-1)D_{50}}}\right]^{\frac{3}{2}} \left[1 - \frac{V_c}{V_m}\right]^4 \quad (2.39)$$

in which V_m = minimum flow velocity for a deposit depth of t/D = 1%.

Regarding alluvial channels, a considerable number of equations for the computation of bedload transport have been proposed. Two methods are listed below for the purpose of exemplifying the parameters involved.

2.3.3.3 Engelund-Fredsøe's mathematical model

$$\Phi_b = 5 \left[1 + \left[\frac{\pi/6\ \beta}{\Theta_b - \Theta_c}\right]^4\right]^{-0.25} \left[\sqrt{\Theta_b} - 0.7\sqrt{\Theta_c}\right] \quad (2.40)$$

in which Φ_b (= $q_b/\sqrt{g(s-1)(D_{50})^3}$) is the transport parameter analogous to that in Eq. (2.36); q_b = bedload transport per unit width [in $m^3/(sm)$]; and β = dynamic friction coefficient (close to 1).

2.3.3.4 van Rijn's semi-theoretical model

$$\Phi_b = 0.053 \frac{T^{2.1}}{D_*^{0.3}} \quad (2.41)$$

where

$$D_* = D_{50} \left[\frac{(s-1)g}{\nu^2}\right]^{\frac{1}{3}} \quad (2.42)$$

in which T is the transport stage parameter as defined in Eq. (2.33); and D_* = particle number.

The parameter ($\Theta_b' - \Theta_c$) represents the excess shear. The methods of Engelund--Fredsøe (1976) and van Rijn (1984A) contain this parameter which is assumed to play a dominant roll in bedload transport.

2.3.4 Author's previous studies

Bedload transport is a complex phenomenon which is difficult to study as a whole. In order to identify different components, the research was done in parts where individual processes could be identified.

2.3.4.1 Stable plane bed

This experimental study was limited to an investigation of the flow in pipe channels over permanently-deposited sediment beds. The beds were stable and plane which means that there was no erosion of the bed and that this had the same slope as the pipe. This implies a fixed, though loose, surface which enables the computation of the flow resistance of the bed using well-known expressions. The only difficulty consists in separating the side-wall effect. In a first study (Perrusquía et al 1986) the side wall elimination procedures of Einstein (1942) and Vanoni-Brooks (1957), using Manning's and Darcy-Weisbach's equations respectively, were applied. In the latter, the friction coefficient, f, corresponding to both bed and walls, was computed using the Colebrook-White equation (Eq. 2.9). In the first series of experiments, sand with a D_{50} = 2.5 mm was used. In an extension of the previous study (Perrusquía et al 1987) spherical marble stones with a D_{50} = 16 mm were used. The experimental apparatus was very similar to the one used in the sediment transport rate measurements reported in this thesis. The experiments were conducted in a 23 m long, 225 mm diameter concrete pipe and the sediment bed covered the whole pipe length.

It was found that the flow capacity of the pipe can be computed using an average bed roughness value corresponding to $k_b = 2.0\ D_{50}$ for the sand bed and $k_b = 1.0\ D_{50}$ for the marble stone bed (see Fig. 2.2). Flows were computed using the composite roughness method of Horton (1937) and Brooks (Vanoni and Brooks 1957).

2.3.4.2 Movable plane bed

Assuming that the flow conditions corresponding to the plane bed without transport are still valid, the flow resistance of the plane bed with transport can be com-

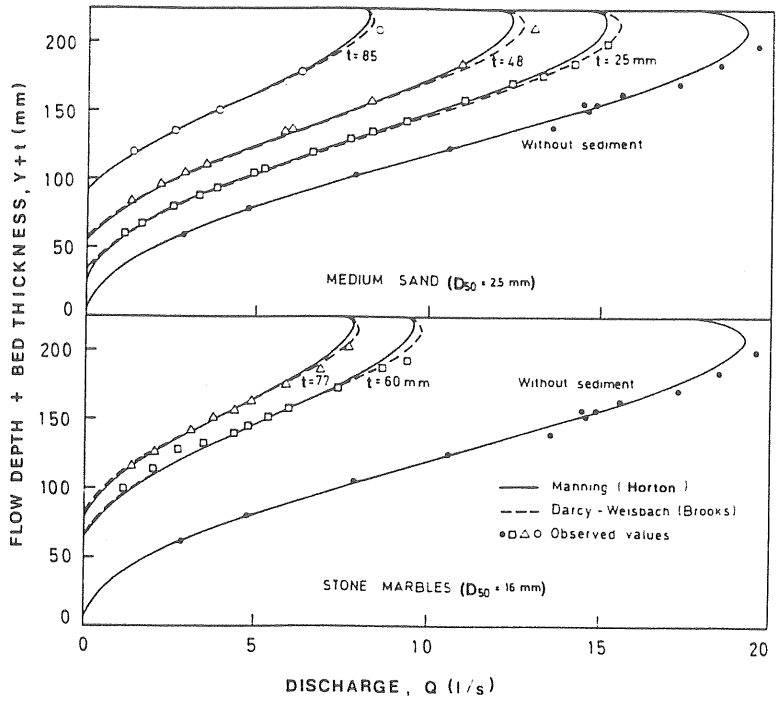

Fig. 2.2 Rating curves for the stable plane beds

puted and compared with the flow resistance of the stable plane bed. All experiments with movable plane beds were made as a part of the experimental program with the movable bedforms which are described in the next section. Flow depths and discharges were selected in such a way that the bed was subject to erosion with no bedforms, i.e. quasi-plane bed condition. Two sand sizes with D_{50} = 0.5 mm and 0.9 mm were used. The results (Perrusquía 1988) suggested that the mean equivalent bed roughness, $\bar{k}_b$, is in the range of approximately 2.0 to 4.5 D_{50}. This can be compared with the value of 2.0 D_{50} for a plane bed with no transport.

2.3.4.3 Movable bedforms

Another series of experiments (Perrusquía 1988) was undertaken to study flow resistance and bedform dimensions in pipe channels with a sediment bed which was laid along the whole length of the concrete pipe. The same sand sizes as mentioned above (2.3.4.2) were used in this case. Discharges and flow depths were increased until bedforms developed along the deposited bed.

The results suggested that the experimental data can be identified in the transitional region between ripples and dunes. Bedform dimensions (height and length) were measured and compared with the values predicted by the methods of Fredsøe (1982) and van Rijn (1984B). Total bed resistance as predicted by the methods of Engelund-Hansen (1972) and van Rijn (1982) was then evaluated. The predicted values were compared with the measured values. The results showed that flow resistance may be predicted to a certain extent using the available methods for alluvial channels.

An extension to this work was made in an attempt to estimate flow resistance in pipe channels with bedforms and to propose an appropriate design method for pipe channels with a sediment bed (Perrusquía, 1990A). Due to the limited amount of data, the need for further work was emphasized and it was recommended that sediment transport measurements should be incorporated in the analysis.

3 FUNCTIONAL RELATIONSHIP FOR SEDIMENT TRANSPORT

The rate of motion of particles in stream traction in a fluid medium contained within the loose bed, pipe walls and free water surface is a function of the flow conditions (flow velocity, depth, energy gradient and acceleration due to gravity), fluid (water density and viscosity) and sediment (density, size and shape) properties, geometric characteristics of the hydraulic section (bed thickness, bed width and pipe diameter) and roughness of sediment and pipe walls. Fig. 3.1 (page 22) shows some of the parameters to be considered in the case of circular channels with a deposited sediment bed. The question that arises is:

Do all these variables significantly affect the transport process ?

3.1 Dimensional analysis

Dimensional analysis is used in this section to define the variables and the functional relationships that govern stream traction in pipe channels. The characteristic parameters that define sediment transport in this kind of flow along with their dimensions are listed in Table 3.1.

Table 3.1 Characteristic parameters for stream traction in pipe channels.

ELEMENT	PARAMETER	SYMBOL	DIMENSION
Flow	depth	Y	L
	energy gradient	S	L/L
	acc. due to gravity	g	LT^{-2}
Fluid	density	ρ	ML^{-3}
	dynamic viscosity	μ	$ML^{-1}T^{-1}$
Sediment	density	ρ_s	ML^{-3}
	size	D_{50}	L
Geometry	bed thickness	t	L
	(total depth)	$(Y+t)$	(L)
	pipe diameter	D	L
Side walls	pipe roughness	k_w	L

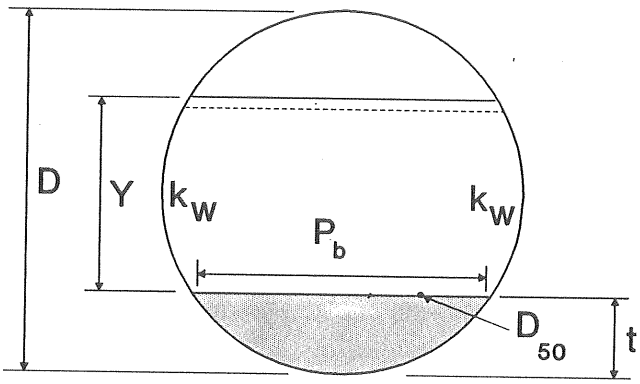

Fig. 3.1 Pipe channel (D, k_w), flow (Y) and sediment bed (D_{50}, P_b, t) parameters

The roughness of the sediment bed, k_b, is included implicitly in the present analysis since it can be described as a function of some of the characteristic parameters. Its determination is part of an iterative procedure presented in Section 5.4. Some of these 10 parameters can be replaced by others which in turn are expressed in terms of the original ones (see Yalin 1972). The new set of characteristic parameters consists of: flow depth, Y, shear velocity, u_*, acceleration due to gravity, g, fluid density, ρ, kinematic viscosity, ν, sediment density, ρ_s, sediment size, D_{50}, sediment bed thickness, t, pipe diameter, D, and pipe roughness, k_w. From the theory for dimensional analysis, sediment transport can be described by a functional relationship including 7 dimensionless variables. The set of 7 dimensionless variables can be expressed in a variety of ways depending on the three characteristic parameters being selected as basic quantities (parameters which have independent dimensions). The combination of these three basic quantities with each one of the remaining seven characteristic parameters gives seven dimensionless power products. The dimensionless version of the transport function is given by the "*π-theorem*" of the theory of dimensions as

$$\Phi_b = f_1(\Theta_b, D_*, s, Z, Y_r, t_r, k_r) \qquad (3.1)$$

where the dimensionless sediment transport is given by the transport parameter:

$$\Phi_b = \frac{q_b}{\sqrt{g(s-1)D_{50}^3}} \tag{3.2}$$

in which q_b = sediment transport rate per unit width (Q_b/P_b).

Eq. (3.2) is identical to the transport parameter that Einstein (1942) proposed using probability and hydrodynamic principles. The dimensionless variables are:

i) Dimensionless bed shear stress

$$\Theta_b = \frac{R_b\ S}{(s-1)D_{50}} \tag{3.3}$$

Θ_b will henceforth be referred to as the Bed Mobility Number.

ii) Particle number

$$D_* = \left[\frac{g\ (s-1)}{\nu^2}\right]^{1/3} D_{50} \tag{3.4}$$

This dimensionless variable has been presented by several authors: Ackers and White (1973) used it for the determination of sediment transport, van Rijn (1984) used it for the classification of bedforms, and Yalin (1985) used it for the estimation of bedform length.

iii) Relative density

$$s = \frac{\rho_s}{\rho} \tag{3.5}$$

iv) Relative grain size

$$Z = \frac{D_{50}}{Y} \tag{3.6}$$

v) Relative flow depth

$$Y_r = \frac{Y}{D} \tag{3.7}$$

vi) Relative bed thickness

$$t_r = \frac{t}{D} \tag{3.8}$$

vii) Relative pipe roughness

$$k_r = \frac{D_{50}}{k_w} \tag{3.9}$$

An alternative expression to Eq. (3.1) is

$$\Phi_b = f_1(\Theta_b, D_*, s, Z, Y_r, \frac{Y+t}{D}, k_r) \tag{3.10}$$

in which the relative total depth, (Y+t)/D, replaces the relative bed thickness, t/D.

This parameter was introduced in the present analysis to evaluate the possible influence of the shape of the hydraulic section, which was divided into trapezoidal, $(Y+t) < D/2$, and concave, $(Y+t) > D/2$.

The functional relationships expressed in Eqs. (3.1) and (3.10) are used to analyze the transport of sediment in pipe channels with a deposited bed. The influence that these dimensionless variables have on sediment transport will be investigated in two ways: 1) individually, to detect the possible qualitative influence of each of them on transport, and 2) simultaneously, to study the dependence of transport on all of them using multiple regression analysis.

4 EXPERIMENTAL STUDIES

4.1 Experimental Apparatus

The experiments were conducted in a 23 m long, 225 mm diameter concrete pipe constructed of 1 m long sections joined by rubber rings. Each section had 800 x 80 mm slots cut in the top. The pipe was placed on a supporting frame and its gradient kept constant for each particular run. The sediment was laid along the invert of the pipe and was then levelled off forming a sediment bed of uniform thickness on a 5 m long test reach in the middle of the pipe's length. There was a 3 m long false floor at each end of the test reach having the same thickness as the loose sediment bed. A layer of sediment with the same grain size as the loose bed was glued to the false floor. A 1 m long PVC pipe was, for observation, placed in the middle of the test reach.

The test rig had recirculating facilities between two tanks, a supply tank and a collecting tank, one at each end of the pipe, with a downstream control tail gate at the end of the pipe. Screens and a conical transition were used at the pipe inlet to minimize disturbance to the flow. An in-line turbine flow meter was installed along the return pipe upstream of the supply tank's inlet. Four piezometers were positioned at four different locations: two on the false floor and two on the loose bed. A 0.2 mm metallic sieve was placed on each piezometer tapping and secured with water proof tape to avoid sand in the piezometer tubes. A point gauge was mounted on a carriage which in turn was placed on rails whose length covered that of the loose bed and one meter of the false floor on each side. An electromagnetic vibrator to supply sediment into the pipe and a specially designed sediment trap were located on top of the upstream false floor and just downstream of the test reach, respectively. See Fig. 4.1 (page 26) for details.

4.2 Methodology

The way that a typical run was carried out is the subject of this section. The detailed measurements as well as the instruments used and their special features are described in Section 4.3.

4.2.1 Experimental procedure

Each run started with a plane, levelled bed, except for selected runs where the sediment bed presented small bedforms from the previous run and where only the flow depth was to be increased as done by other researchers (Lau 1989). Prior to

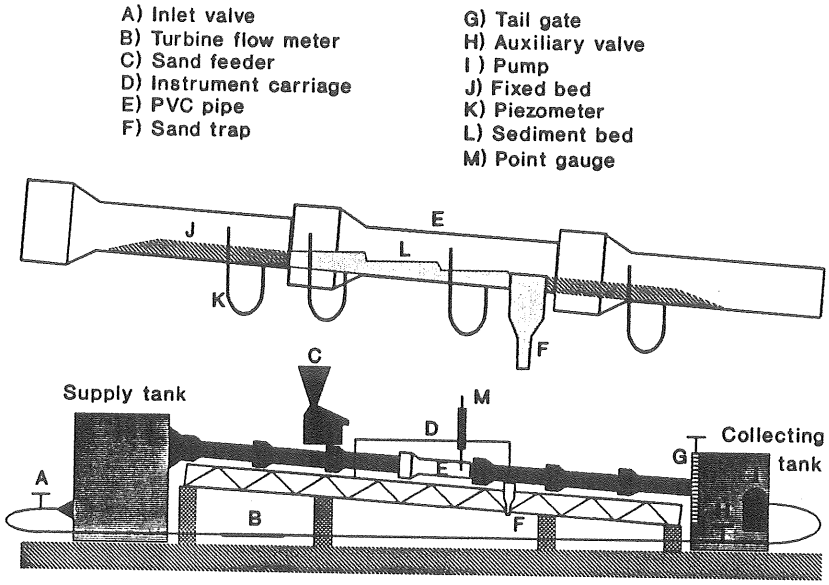

Fig. 4.1 Layout of the experimental apparatus

each run, the tail gate was completely closed and the pipe slowly filled with water from the downstream end up to a half-full level at the upstream end of the test reach. The pump, located inside the collecting tank, was started and the valve at the inlet of the upper tank opened just enough to establish a small flow of water along the pipe. The tail gate was then carefully opened to avoid any spillage since the pipe had slots all along. The opening of both the valve and the tail gate was systematically repeated until the desired uniform flow was achieved. Readings of the water surface elevation were made at first using all four piezometers until the flow depth was considered almost constant. Finally, direct measurements were made using the point gauge along the pipe. This was possible because the water surface was relatively steady. The water surface slope, S_w, was then determined and compared with the pipe slope, S_o. The manipulation of both the valve and the tail gate continued until $S_w \cong S_o$. In the cases where this was not possible, a nonuniform flow correction was used for the water surface slope. Flow discharge rate was recorded as well as water temperature.

Even before uniform flow conditions were achieved, erosion started at the surface of the sediment bed. The sediment feeder was started to compensate for the sediment being transported downstream and to maintain equilibrium. This was

done on a trial basis and the rate of supply was gradually increased as the flow approached uniform conditions. There were two control sections, one at each end of the loose sediment bed, to observe whether scour or aggradation of the bed occurred. If so, the rate of supply was adjusted. In the meantime, bedforms developed along the whole test reach. Continuous checks on flow discharge rate, flow depth, water temperature and rate of sediment supply were made to keep their values nearly constant. This process was continued for one hour before proceeding to take samples through the sediment trap. Water temperature was kept constant from the moment uniform flow was established. Fluctuations were kept within $\pm 1.0^{o}$ C by introducing fresh water into the system. The first sample was taken and its weight immediately converted from wet to dry in order to compare the latter with the weight of dry sediment supplied by the feeder. The dry weight of the first sample gave the first indication on whether equilibrium had been established between the rate of supply and the rate at which the sediment was falling into the sediment trap. It took one to two samples before equilibrium was accomplished. Several samples were taken and their rates compared with the rates of supply.

After the last sample had been taken, the tail gate, the valve at the inlet of the supply tank and the pump were all shut off in that order. First the tail gate to create a backwater curve hence decelerating the flow leaving the bedforms intact. The water was then slowly drained from the pipe overnight. The following day, bedform dimensions were measured using a specially designed automatic bed follower mounted on a carriage that could move on the same rails as the point gauge. The longitudinal sediment bed profile was traced along the pipe's centerline.

A few velocity measurements were performed using a micro-propeller current meter. Both cross-sectional and vertical profiles were measured along the sediment bed. These measurements were made both during and after the sampling. In some selected runs with bedforms, the sediment bed was "frozen" using rapid setting cement which apparently did not modify the roughness of the sediment bed while maintaining the geometry of the bedforms (see 4.3.7). By doing so, the current meter could be lowered close to the bed. These particular measurements were made after bedform dimensions had been measured and the day after the cement had been applied to the sediment bed along the whole test reach.

4.2.2 Sediment properties

The sediment used for the experiments was uniformly-graded sand. Two different sizes were tested: D_{50} = 0.9 mm and D_{50} = 2.5 mm. Both sands were quartz with a relative density, s = 2.65. Sieve analysis was carried out as soon as the sand arrived at the laboratory and during the course of the experiments to check whether pulverization of the particles occurred. The analysis was carried out on different layers in the sediment bed to see if there were significant variations in particle size between the material composing the sediment bed and the material being transported. The grading curves are shown in Figs. 4.2 and 4.3.

4.2.3 Reproducibility tests

Some runs were repeated starting from a plane bed under similar flow conditions to verify the reproducibility of both the bedform dimensions and the sediment transport rate. A comparison for run 8 is shown in Table 4.1. The variation is considered to be acceptable.

Table 4.1 Reproducibility of run 8 (D_{50} = 0.9 mm and t = 90 mm).

Date	1989-04-24	1989-04-26
Depth	51 mm	50 mm
Velocity	0.352 m/s	0.359 m/s
Bedform height & length	2 & 226 mm	3 & 247 mm
Sediment transport rate	37 g/min	38 g/min

4.3 Measurements

This section is intended to describe how the specific measurements were performed including the operation of the instruments and equipment. Other electronic instruments and devices required for the calibration and operation of the principal instruments are not discussed in this report.

4.3.1 Flow discharge rate

Flow discharge rates were measured using a turbine flow meter (TFM) which consisted of a turbine inserted in the middle of a 50 mm diameter steel pipe which expanded to 100 mm on both sides. The steel pipe section was in turn

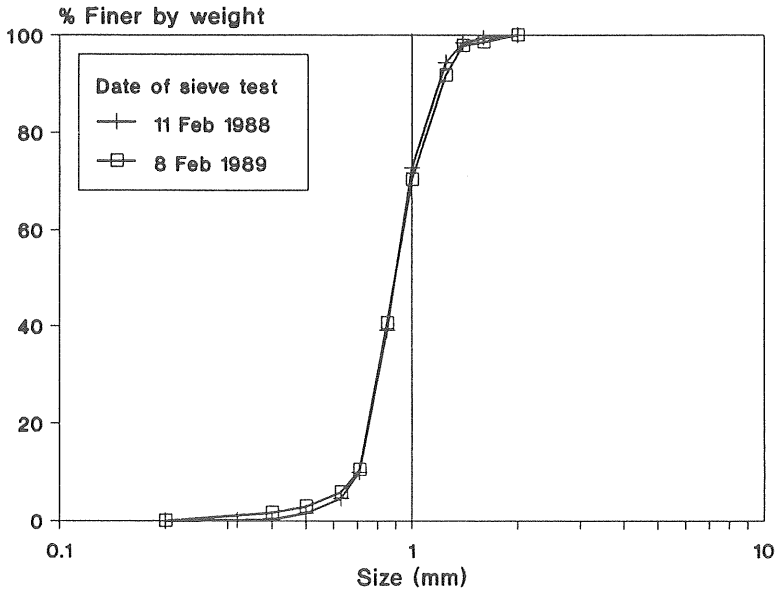

Fig. 4.2 Grading curves of sand D_{50} = 0.9 mm

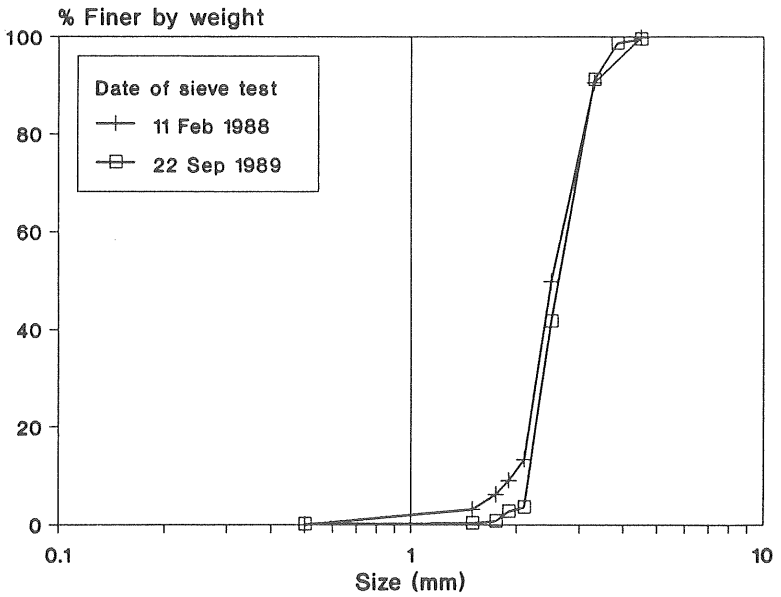

Fig. 4.3 Grading curves of sand D_{50} = 2.5 mm

connected to the recirculating pipe as shown in Fig. 4.4. The output signal from the TFM was sent to a counter unit that gave a reading in pulses per second. The manufacturer's calibration curve (accuracy of 0.5 % for the range 2.0 l/s $\leq$ Q $\leq$ 20.0 l/s) was used. Some independent tests were carried out using a volumetric flow meter that was permanently connected to the system immediately downstream of the inlet valve. The maximum variation between both flow meters was of 3.7% and 1.5% for the lower and upper limits respectively. Each experiment was started by turning on the pump. This produced a sudden increase in pressure all along the recirculating pipe. To avoid any damage to the TFM, an auxiliary valve was installed at the outlet of the collecting tank. This valve together with the one at the inlet of the supply tank were opened and operated simultaneously to set a particular discharge. Once uniform flow conditions had been achieved, a series of ten consecutive readings were taken from the counter unit which recorded the mean value in pulses per second for a 10 s period. This procedure was repeated periodically to keep the flow discharge rate constant during the run. To ensure that only clear water circulated through the TFM, a dividing wall was built in the middle of the collecting tank to prevent any sediment from entering the pump. Finally, the auxiliary valve was shut off before the pump for the same purpose of avoiding any damage to the TFM.

4.3.2 Flow depth

As mentioned in 4.2.1, the piezometers were used to obtain a first approximation of the constant flow depth, while the point gauge was used to define the water surface slope. The copper piezometer tappings were 5 mm in diameter and connected to transparent plastic tubes. The zero value on the millimetric scale of each piezometer was set at the corresponding elevation of the pipe invert. The point gauge consisted of a 60 cm long graduated scale with a vernier. It was mounted on a carriage which in turn was placed on rails. It was moved along the centerline of the pipe. See Fig. 4.1 (page 26) for the location of the piezometers and the point gauge. Since the sediment bed thickness, t, was known, the flow discharge rate, Q, was selected so that the total depth (Y+t) was: 1) below half-full [Y+t < D/2], 2) half-full [Y+t = D/2], or 3) above half-full [Y+t > D/2], D being the pipe diameter. Each time the valve and the tail gate were simultaneously opened to achieve uniform flow, a series of readings of the total depth (t+Y) were recorded on the scale of the piezometers. The readings were made to the nearest 0.5 mm. A difference of $\pm$1.0 mm between the reading at each piezometer was allowed before proceeding to use the point gauge.

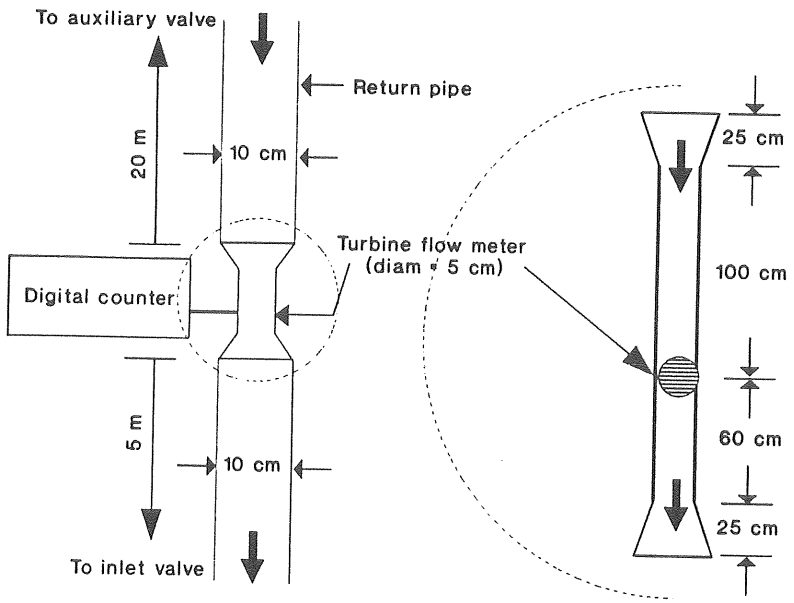

Fig. 4.4 Schematic layout of TFM

This was possible because the water surface was fairly stable for the range of total depths tested. Standing waves were present for total depths where $Y+t > 0.85\ D$ and this was the case only in one run. Each time these readings were taken, a linear regression was carried out to determine the slope of the water surface, S_w. Fine adjustments to the opening of the tail gate were made and the process of reading water surface elevations and calculating water surface slopes was repeated until the latter and the pipe slope, S_o, agreed to within a ±5.0% difference.

4.3.3 Flow velocity

Flow velocities were measured with a 10 mm diameter micro-propeller current meter which was mounted on a carriage and on the same rails as the point gauge. It could be moved both along and across the bed. Similar to the TFM, the current meter was connected to a counter unit that gave readings in pulses per second. The current meter was calibrated for the range $0.1\ m/s \leq V \leq 0.9\ m/s$. The calibration was made in the laboratory by mounting the current meter on a carriage which moved along an 80-m long flume at constant speeds. The regression equation for this particular range was considered practically linear with a standard error of 0.75 cm/s and a regression coefficient of 0.99 as was the case for a

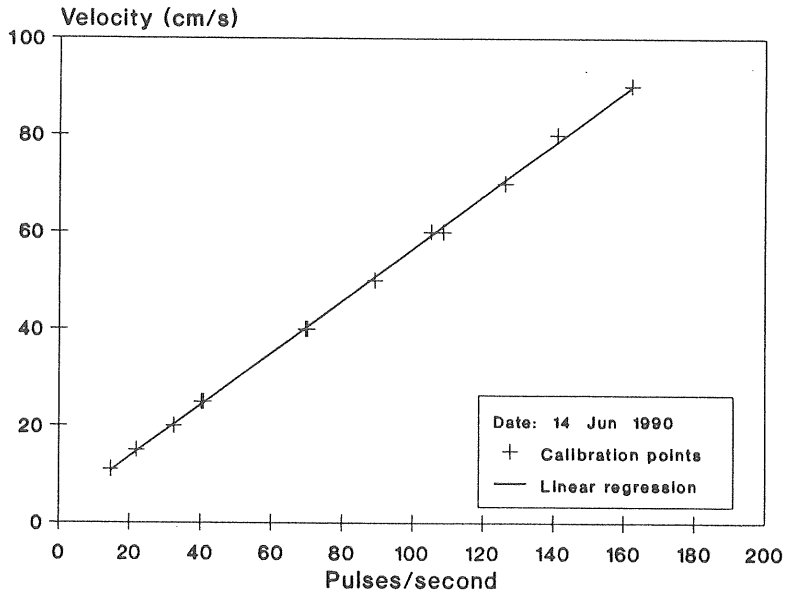

Fig. 4.5 Calibration for current meter

typical calibration shown in Fig. 4.5. Calibrations were done periodically throughout the experiments to check whether the current meter's performance had been affected by dirt or any other foreign particles. While not in use, it was kept submerged in distilled water.

The velocity measurements were done after the samples had been taken, the system still being in equilibrium, i.e. both the fluid and the sediment transport are constant. The measurements covered two conditions: 1) loose sand beds with and without bedforms, and 2) fixed sand beds with bedforms.

In the first condition, the measurements were aimed to determine the pattern of velocity distribution in the cross section. Velocities were taken at a minimum of six points along the vertical and at three to four points across the section. The micro-propeller could not be lowered too close to the sediment bed because the sand particles obstructed the propeller making the measurements uncertain.

In the second condition, the purpose was to determine both the pattern of velocity distribution in the cross section and the vertical velocity profile in the centerline at several sections along a bedform. Velocities could be measured a few millimeters

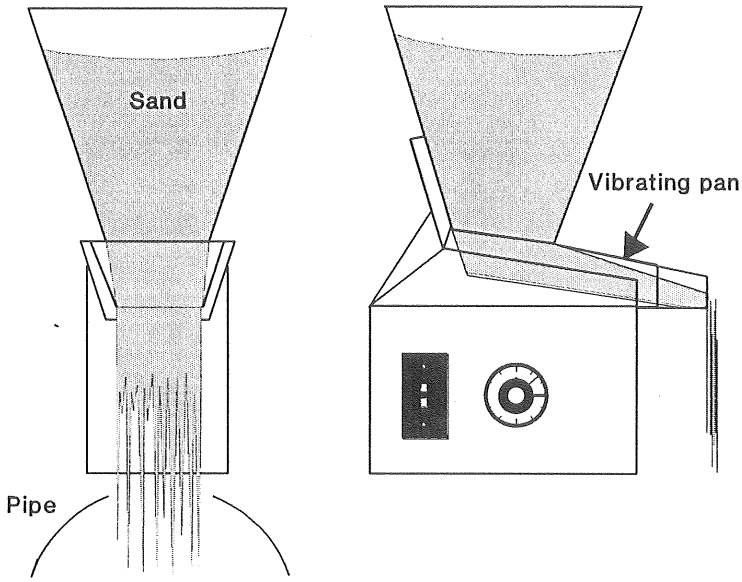

Fig. 4.6 Schematic diagram of electromagnetic vibrator

from the sediment bed surface. In any event, a series of ten consecutive readings were taken from the counter unit which recorded the mean value in pulses per second for a 10 s period. The corresponding velocity was obtained from the calibration curve.

4.3.4 Sediment supply rate

A sediment feeder was used to supply material into the pipe. The feeder was driven by an electromagnetic vibrator which is built into an enclosed housing together with an on-off switch and a potentiometer to give variable control over the capacity. See Fig. 4.6 for a schematic description of the feeder. The sediment feeder was turned on as soon as erosion of the sediment bed ocurred. The actual rate of supply was not measured during the process of achieving uniform flow.

It was only estimated from the calibration curve because at this stage, to know the exact rate of supply was irrelevant. It was not until both the rate of supply and the sediment being eroded from the surface of the bed were considered to be in a preliminary state of equilibrium that the former was measured by collecting the sand, which was conveyed by the vibrating pan, before it entered the pipe for a

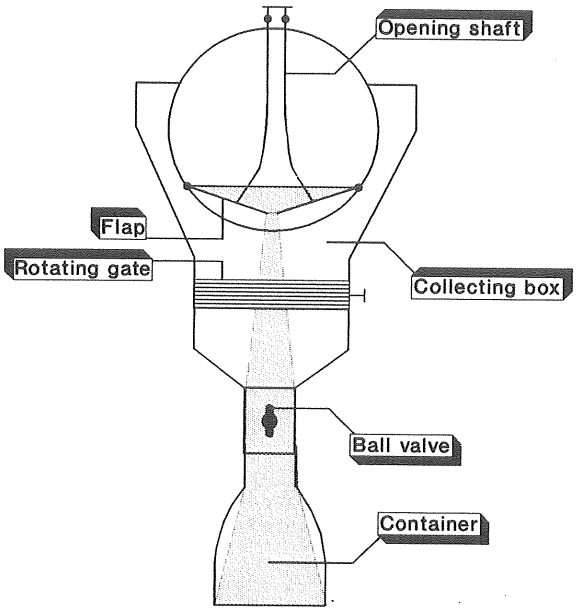

Fig. 4.7 Cross section of the sediment trap

one-minute period. The rate of supply was always compared with the rate at which the sediment was falling into the sediment trap and, if needed, adjusted until equilibrium between these two rates was accomplished.

4.3.5 Sediment transport rate

The collection of the sediment being eroded off the bed was made by means of a trap. This consisted of a flap box constructed of PVC. The opening for the trap was 50 mm wide and its lateral dimension was adjusted depending on the thickness and width of the sediment bed. It was located just downstream of the test reach. Other components of the trap are: opening shafts, flaps, rotating gate, collecting box, ball valve and container (see Fig. 4.7). The sediment trap was not opened until the preliminary state of equilibrium mentioned above had been reached. Several samples were taken. The sampling time was selected depending upon the intensity of the transport. For low transport rates the sampling time was up to 60 min, while for high rates between 10 to 15 min for each sample. At least three samples were taken consecutively before closing the sediment trap. In some runs, the sediment trap was reopened after a period of 30 to 60 min to take two more samples. The weight of each individual sample was converted from wet to

dry directly after each sampling. The purpose was to have a quick reference for comparison between the dry weights of both the sample from the sediment trap and the sand supplied by the feeder. However, the samples were always dried in the oven and weighed the next day. The sediment discharge was taken as the mean value of all samples taken in grams per minute. The procedure to collect the samples was as follows:

Both the rotating gate and the ball valve were opened to allow water to enter the trap. Once the trap was full of water, the flaps could be opened by pushing down the opening shafts to start collecting sediment. After a selected period of time, the rotating valve was closed first followed by the ball valve. When all the sediment was deposited in the container, this was disconnected from the system and replaced by a container full of water. In the meantime, the collection of sediment had not been interrupted so that the rotating gate was reopened to carry on with the next sampling. After the final sample was collected, the opening shafts were pulled up to return the flaps to their original position.

4.3.6 Bedform geometry

A specially designed instrument was used to trace the longitudinal sediment bed profile along the centerline of the pipe. From such profiles, bedform dimensions could then be determined. The instrument was mounted on a carriage which in turn was placed on rails whose length covered that of the loose bed and one meter of the false floor on each side. The moving mechanism on the carriage had horizontal motion at a speed of about 1.0 mm/s. Periodical calibrations were made to confirm that this speed was constant. The bed follower was basically a point gauge with a moving mechanism in the vertical direction. Both the point gauge and carriage were connected to a data acquisition and control (DA&C) system. A specially developed computer program instructed the point gauge to descend until the tip touched the sediment surface, to ascend a couple of millimeters and to repeat the movement up and down until the carriage came to the end of the reach. Every contact with the sediment surface was transmitted as a signal to the DA&C system which converted the input data to coordinates. The result was a longitudinal bed profile which could be plotted and statistically analyzed. The bed follower is illustrated in Fig 4.8 (page 36).

The program that controlled the movement of both the carriage and the follower, rotated the system of coordinates from horizontal to the actual pipe slope. The carriage was placed manually at each pipe section along the test reach.

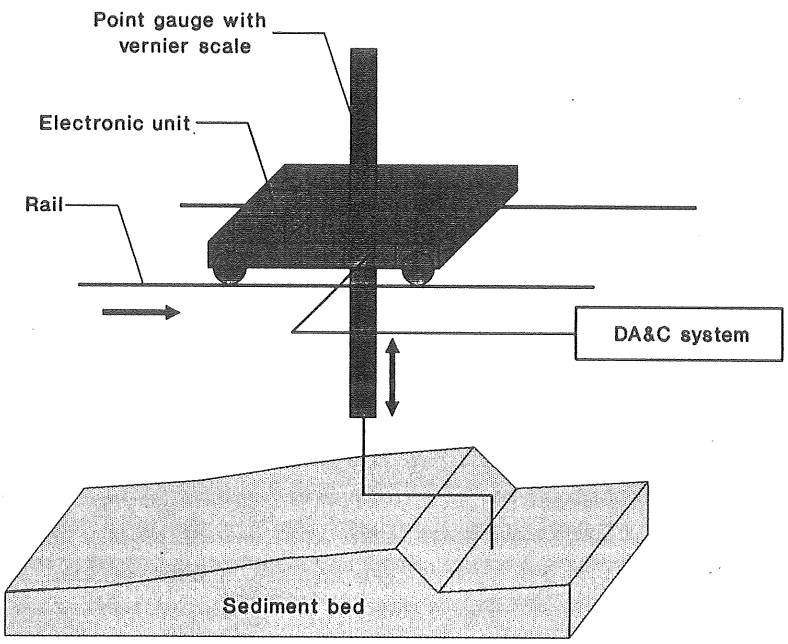

Fig. 4.8 Schematic diagram of bed follower

The program was run and the procedure is described below:

1) The carriage took its start position at each pipe section.
2) The point gauge descended to touch the sediment surface.
3) The file that was assigned a name.
4) The pipe section was given.
5) The pipe slope was given.
6) The length of each pipe section as well as the joints between pipes had previously been stored in the program.
7) The initial values for the X-Y coordinates were recorded.
8) The measurement started. The X-Y values were recorded with a frequency of about 1.0 Hz.
9) The carriage reached the end of the pipe section and the point gauge ascended to a given position while the computer showed the distance travelled by the bed follower. This distance and the length of the corresponding pipe section should be identical. The carriage was moved manually to the next pipe section and the procedure repeated.

The point gauge could be shifted from a downstream to an upstream position to measure the sediment profile along the joints between the pipes. In that way, a longitudinal bed surface profile of the entire length along the test reach could be plotted. Bedform height was determined using the technique described by Vanoni and Hwang (1967) as the difference in elevation between the crest and the mean of the elevations of the troughs at the ends of the bedform.

4.3.7 Shear stress

As already mentioned in 4.2.1, velocities were measured in the centerline at several sections along "frozen" bedforms. It was also stated that the roughness of the sediment bed had not been modified after the application of the fast-hardening cement. This was corroborated by the fact that the flow conditions could be reproduced after the bedforms had been fixed. The purpose of these measurements was to obtain vertical velocity profiles which in turn could be used to indirectly determine the bed shear stress according to the procedure described in 2.2.1.

5 ANALYSIS OF EXPERIMENTAL RESULTS

The data reported in this chapter belong to the experiments conducted at Chalmers (Chalmers series). Two additional series of experiments were performed at the Department of River Engineering, Hydraulics Research Ltd. (Wallingford series) and at the Department of Civil Engineering, The University of Newcastle upon Tyne (Newcastle series), both in England. The data have been published earlier in a separate report (Perrusquía 1990B) and were used in the present analysis. The purpose of these additional experiments was to extend the range of application of the main series (Chalmers series) by testing different pipe diameters, pipe materials, sand sizes and sediment bed thicknesses. Sediment transport rates and bedform dimensions in part-full pipes with a deposited bed were measured.

The experimental data range is summarized in Table 5.1. A complete tabulation of each particular run is presented in the Appendix. The pipe material was concrete with a diameter of 225 mm, the sand used was quartz with a relative density of 2.65 and the water temperature was maintained around 20° C.

Table 5.1 Range of the experimental data.

Run No.	Pipe Slope S	Sand Size D_{50} (mm)	Sediment Bed Thickness t (mm)	Sediment Bed Width P_b (mm)	Flow Depth Y (mm)	Flow Discharge Q (l/s)
1-10	$2x10^{-3}$	0.90	90	220.5	20-89	0.49-7.50
11-19	$3x10^{-3}$	"	"	"	18-100	0.83-10.7
20-27	$4x10^{-3}$	"	"	"	15-64.5	0.81-7.0
28-36	"	2.50	"	"	40-104	3.0-11.0
37-43	$5x10^{-3}$	"	"	"	29-89	3.0-11.0
44-47	"	"	45	180.0	44-115	4.35-16.1
48-50	$4x10^{-3}$	"	"	"	52-83.5	4.50-10.5
51-53	$6x10^{-3}$	"	"	"	42-90	4.15-12.1
54-56	$2x10^{-3}$	0.90	"	"	65-107	5.95-12.2
57-58	$3x10^{-3}$	"	"	"	50-67.5	4.37-7.33

In the Wallingford series, the pipe material was concrete with a diameter of 450 mm and the sand had a mean size of 0.72 mm and a relative density of 2.65. A total of nine runs were done with a pipe slope in the range 0.001 to 0.004 and a relative sediment depth (t/D) of 0.18.

In the Newcastle series, the pipe was made of PVC with a diameter of 154 mm. The sediment used was sand with a mean size of 1.0 mm and a relative density of 2.59. A total of eleven runs were done for a pipe slope in the range 0.002 to 0.004 and a relative sediment depth (t/D) of 0.27. The results from both series are reported in this chapter in the sections dealing with resistance, bedform and sediment transport.

5.1 Velocity profiles

A total of five velocity measurements were made during the experimental program. Of these, three were on loose sand beds while two were on fixed sand beds. The measurements were made in the middle of the 5 m long test reach. Table 5.2 provides a brief description of the conditions tested.

Table 5.2 Conditions for the velocity measurements.

Run No.	BED SURFACE			Bed Configuration	Centerline profiles	Cross section
	Loose Bed	Fixed Bed	False Floor			
6	YES		YES	Movable, plane	3	
8A†	YES			Bedform	1	1
43		YES		Bedform	1 (crest)	
48	YES			Movable, plane	1	
58		YES		Bedform	6	1 (crest)

† This run was specially made for cross-section velocity measurements.

Figs. 5.1 and 5.2 illustrate the velocity distribution in the cross-section for runs 8A and 58, both having a bed configuration with bedforms. The patterns of velocity

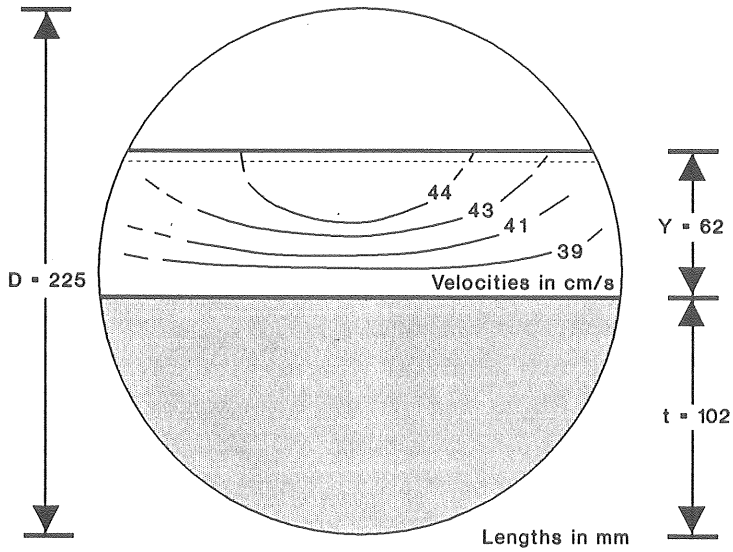

Fig. 5.1 Velocity distribution in the cross section for run 8A

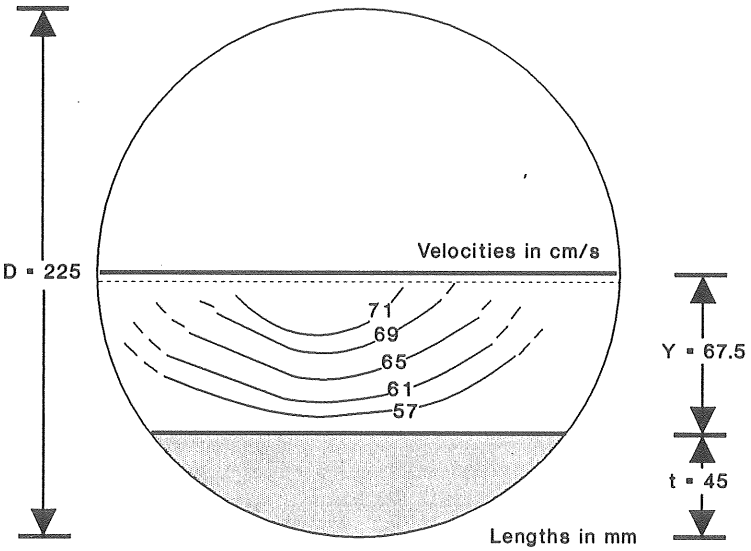

Fig. 5.2 Velocity distribution in the cross section for run 58

distribution in the cross-section show the same tendency for a zone of maximum velocity close to the center. This could not be defined in detail due to the limited amount of measured points close to the free surface. The patterns are asymmetrical probably due to irregular bedforms and other irregularities.

The vertical velocity profile in the centerline for run 6 is shown in Fig. 5.3 while in Fig. 5.4, the logarithmic velocity-defect profile is plotted according to the procedure described in 2.2.1. It can be seen that the velocity distribution follows fairly well the logarithmic law expressed by Eq. (2.6). The measurements for run 6 were made on a movable, plane sediment bed.

Fig. 5.5 (page 44) shows that for run 48 the measured maximum velocity, u_{max}, occurred below the free surface which agrees with what is reported in the literature for open channels (Chow 1959). Fig. 5.6 (page 44) confirms the same findings reported in run 6 regarding the logarithmic velocity distribution.

Velocity profiles obtained with bedforms are showed in Figs. 5.7 to 5.10 (pages 45-46). Figs. 5.7 and 5.8 correspond to run 43 whereas Figs. 5.9 and 5.10 to run 58. In run 43, velocities were measured at a section half the distance between trough and crest and exclusively at the centerline. In run 58, vertical velocity profiles were measured along the bedform (see Fig. 5.11, page 47) and at a distance of 30 mm on either side of the centerline at the crest.

The results are quite similar for all four runs (6, 48, 43 and 58, which are considered typical and representative of the present study) even though their bed and flow conditions are different. Attention should be drawn to the fact that vertical velocity profiles measured along the centerline of the channel give the highest flow velocities. In summary, it appears that the velocity-defect law can be used to describe the vertical velocity distribution for the conditions presented in this experimental study.

5.2 Hydraulic radius of the sediment bed

Shear velocities were obtained from Figs. 5.4, 5.6, 5.8 and 5.10 as the slope of the corresponding regression line. These values were used to determine both bed shear stress, τ_b, and hydraulic radius of the bed, R_b. Table 5.3 lists the experimentally determined R_b values and those estimated using side wall elimination.

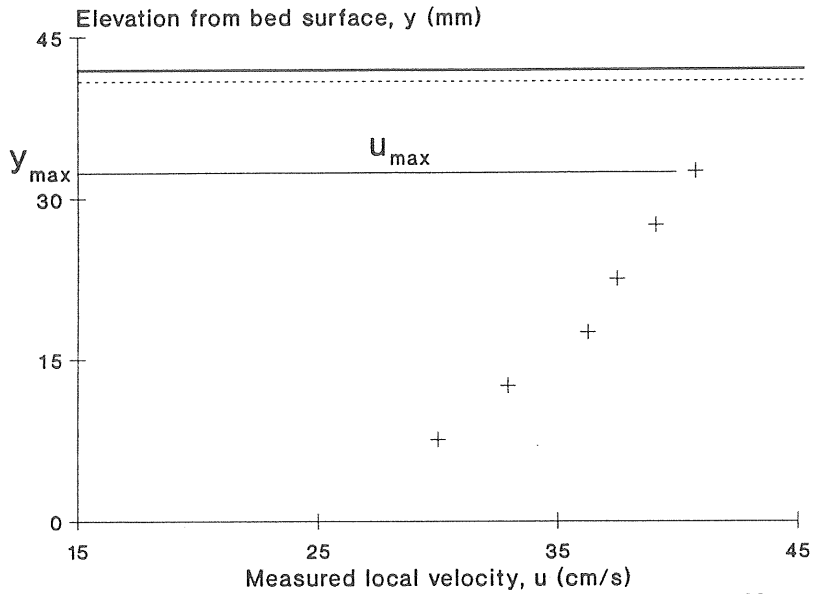

Fig. 5.3 Vertical velocity profile through the centerline for run 6 (t = 90 mm)

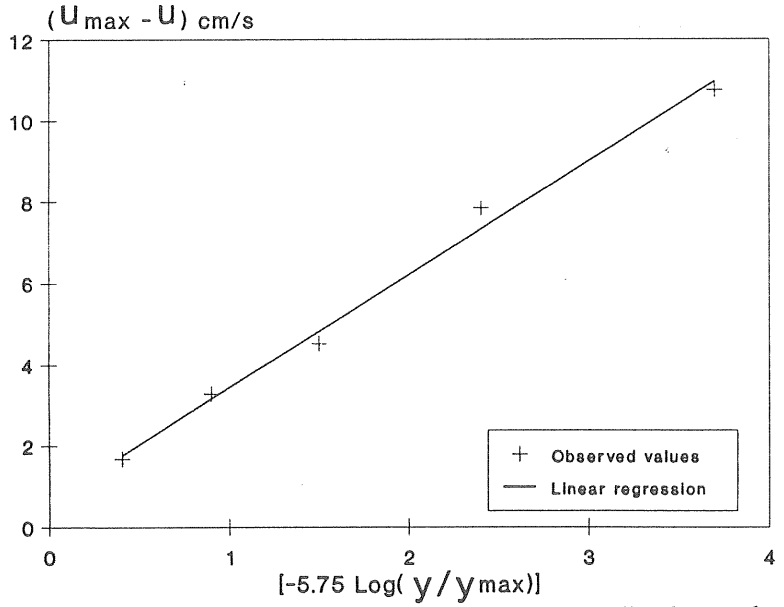

Fig. 5.4 Logarithmic velocity distribution through the centerline for run 6

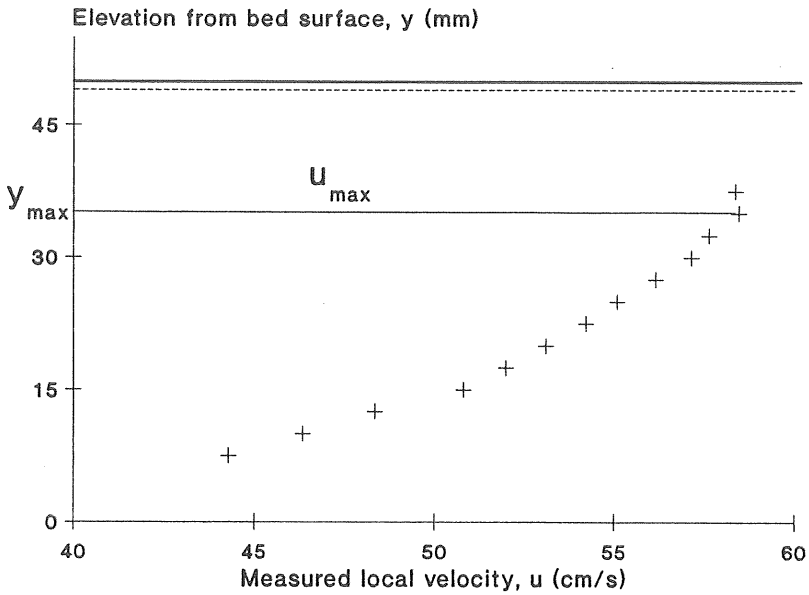

Fig. 5.5 Vertical velocity profile through the centerline for run 48 (t= 45 mm)

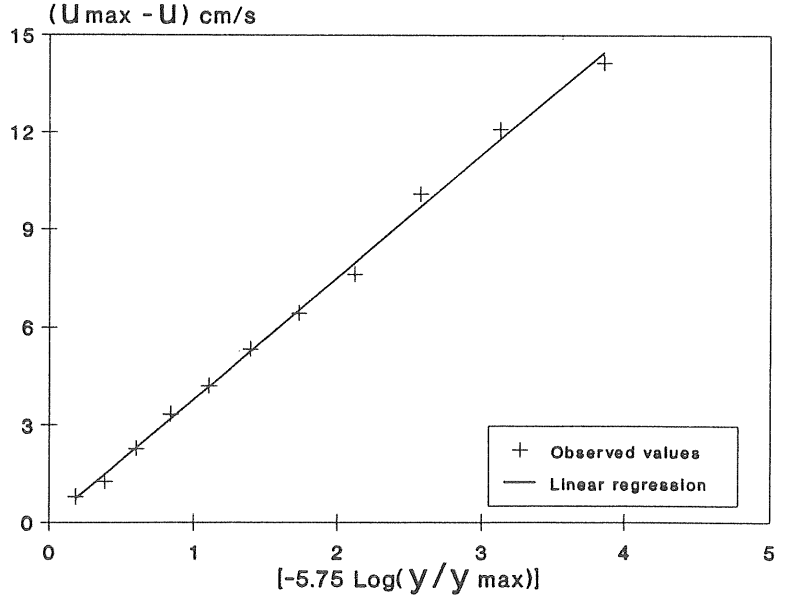

Fig. 5.6 Logarithmic velocity distribution through the centerline for run 48

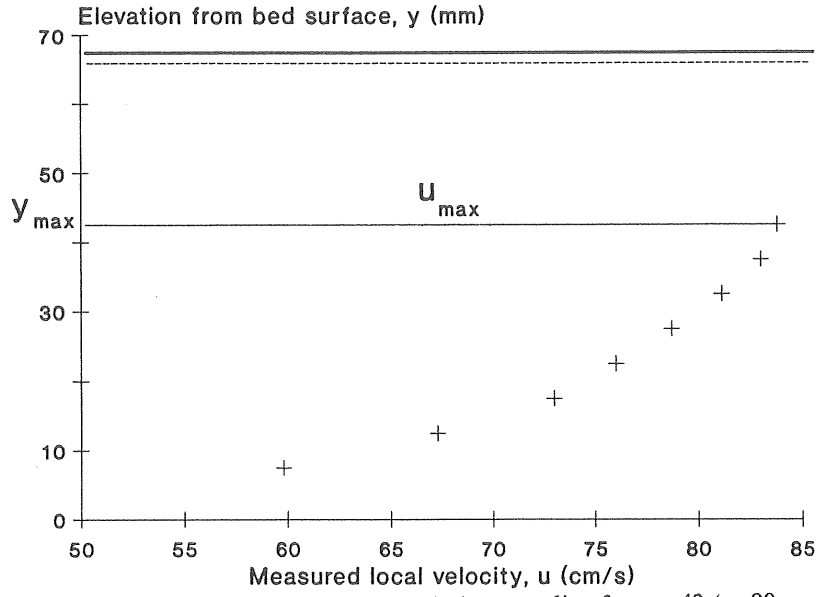

Fig. 5.7 Vertical velocity profile through the centerline for run 43 (t= 90 mm)

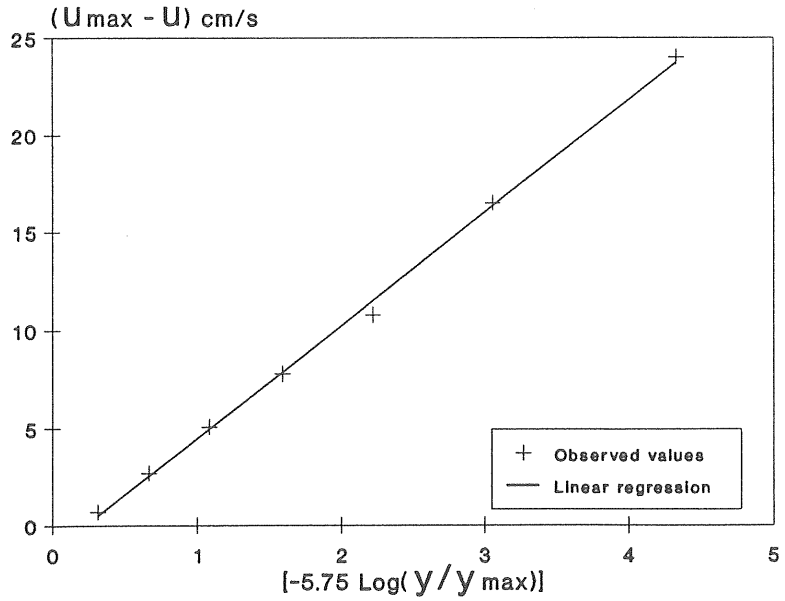

Fig. 5.8 Logarithmic velocity distribution through the centerline for run 43

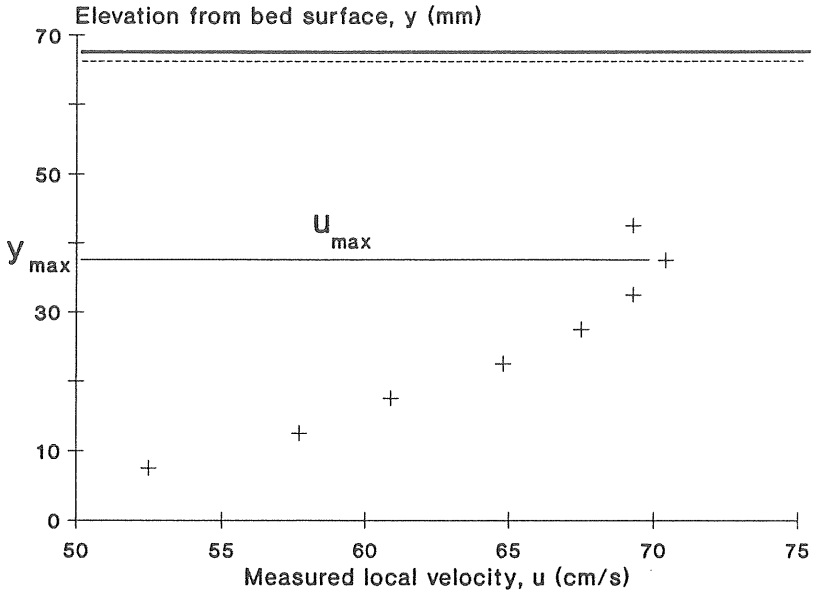

Fig. 5.9 Vertical velocity profile through the centerline for run 58 (t= 45 mm)

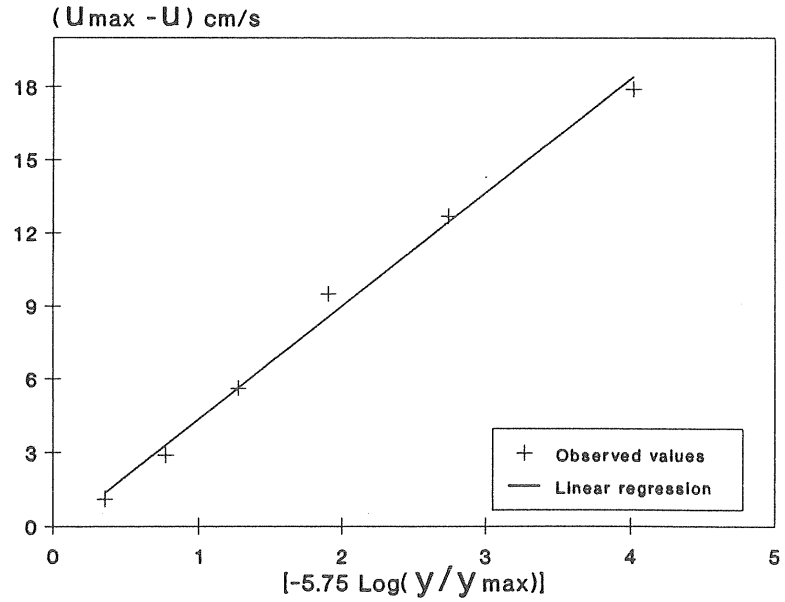

Fig. 5.10 Logarithmic velocity distribution through the centerline for run 58

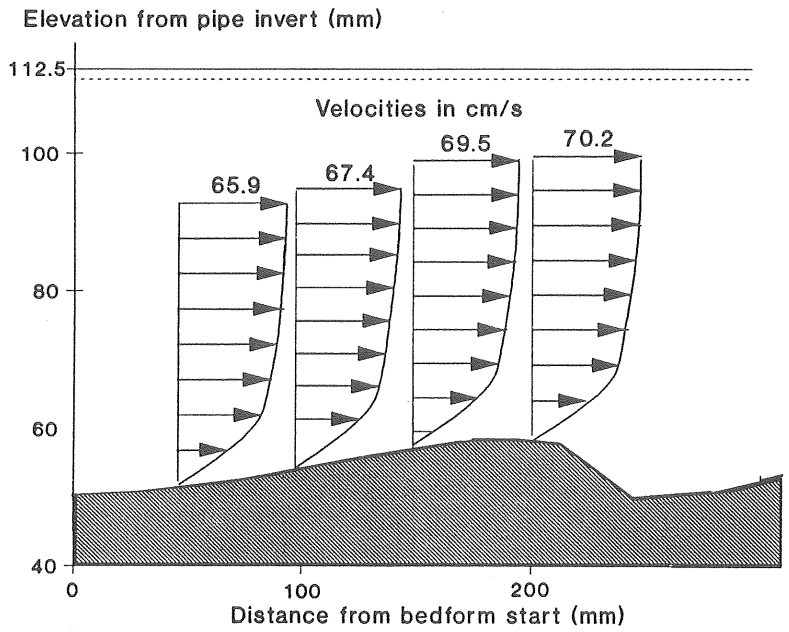

Fig. 5.11 Velocity profiles along the bedform for run 58

Table 5.3 Comparison between experimental and calculated R_b.

Run No. Bedform condition	Hydraulic radius of the sediment bed, R_b (mm) Side wall elimination technique (mean) Einstein	Vanoni	Velocity profile measurements (exper./estim.)
6 Movable, plane bed	35	36	40(+13%)
43 Fixed bedform, halfway	66	67	68(+2%)
48 Movable, plane bed	48	49	39(-24%)
58 Fixed bedform, at crest	55	57	74(+32%)
58 150 mm upstream crest	55	57	70(+25%)
58 Mean of 3 profiles	55	57	59(+5%)
58 Mean of 6 profiles	55	57	65(+16%)

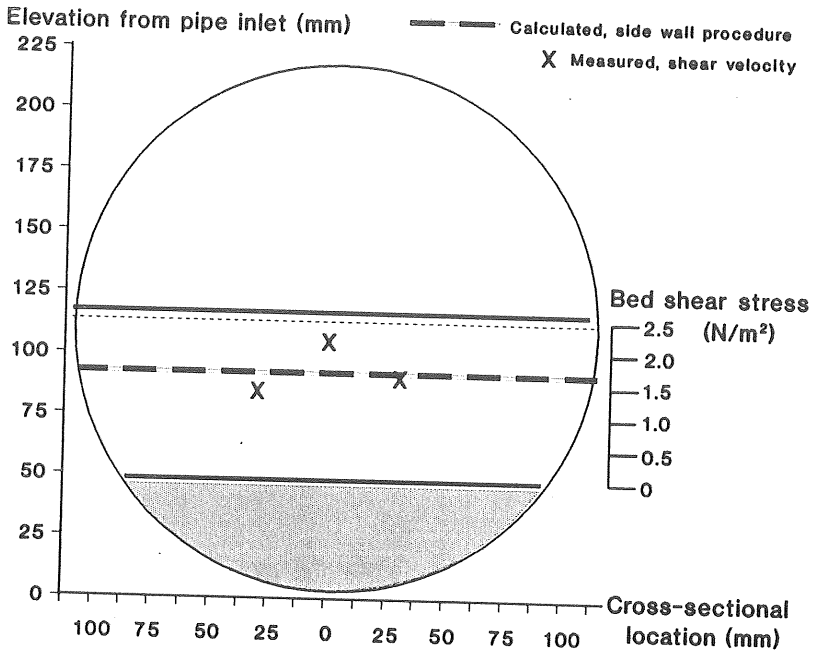

Fig. 5.12 Bed shear stress distribution for run 58

The values of R_b in run 58 are given in Table 5.3 for single profile measurements, taken at the crest and 150 mm upstream the bedform crest, for three profiles taken across the crest and for six profiles taken at four points along the centerline and one point on each side of the bedform crest. The mean value, obtained from three observations (59 mm), does not differ significantly from the calculated value (56 mm). Both the measured and calculated bed shear stresses at the crest for run 58 are plotted in Fig. 5.12. The largest bed shear stress occurred, as expected, in the centerline. The average value of the measured bed shear stress was 1.75 N/m^2, which can be compared with 1.65 N/m^2, the mean value obtained using the side wall elimination procedure.

The agreement between the measured and the estimated values is fairly good considering the following facts: 1) the value of the bed shear stress, τ_b, determined from velocity profiles exclusively along the centerline, is higher than the calculated one obtained from side wall elimination, 2) if several profiles across the crest are available, as is the case for run 58, the average value agrees fairly well with the calculated one, and 3) a fluctuation of $\pm$ 5% in τ_b corresponds to the same variation in the hydraulic radius of the bed, R_b, which may be considered to be acceptable for engineering purposes.

It can be concluded that the side wall elimination procedures of Einstein and Vanoni can be used to estimate the hydraulic radius of the bed for the present flow conditions.

5.3 Critical mobility

Table 5.4 summarizes the conditions for the runs used to establish the critical mobility number for both sand sizes. In Figs. 5.13 and 5.14 (page 50), the bed mobility number is plotted against the volumetric concentration.

Table 5.4 Conditions for the critical shear measurements.

	D_{50} = 0.9 mm			D_{50} = 2.5 mm	
Run No.	Bed configuration	Slope ($x10^{-3}$)	Run No.	Bed configuration	Slope ($x10^{-3}$)
4,6,7	Plane	2	30-31	Plane	4
8	Irregular	2	32-33	Irregular	4
13-14	Plane	3	48-49	Plane	4
15-16	Irregular	3	40-42	Irregular	5
22-23	Plane	4	44	Plane	5
24-25	Irregular	4			

In Table 5.4, "irregular bed" implies a bed surface which, although not exactly plane, has not reached any identifiable bedform condition. The points in Figs. 5.13 and 5.14 were plotted for each particular slope. They show a tendency to meet at approximately the same critical value, which was selected as the value corresponding to a volumetric concentration of 1 ppm for the line referred to as the "Envelope line". The experimental critical mobility numbers for both sand sizes are plotted in Fig. 5.15 (page 51) together with Shields' curve. Both values of the critical mobility number, Θ_c, lie close to the curve. This means that the traditional way of estimating the shear stress for the initiation of motion using Shields' diagram may be used in the case of pipe channels and for the present sand sizes with good approximation.

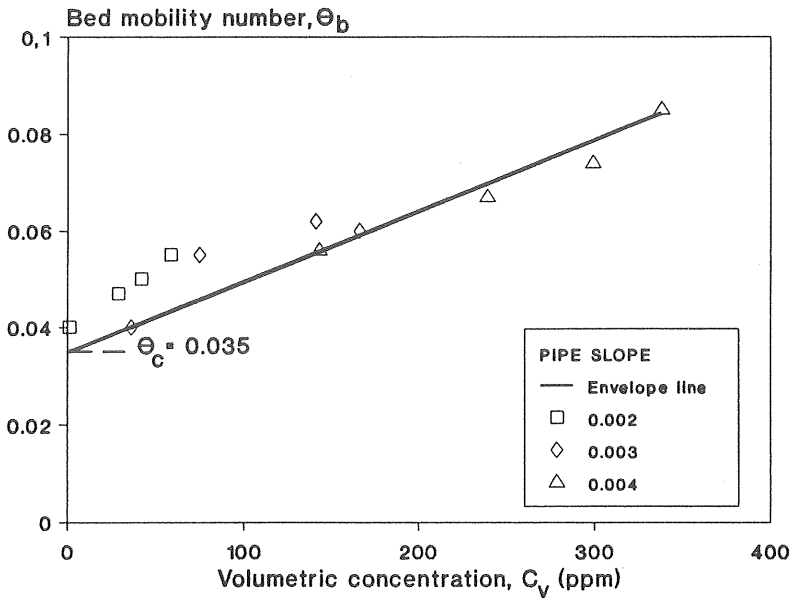

Fig. 5.13 Critical mobility number for sand size D_{50} = 0.9 mm

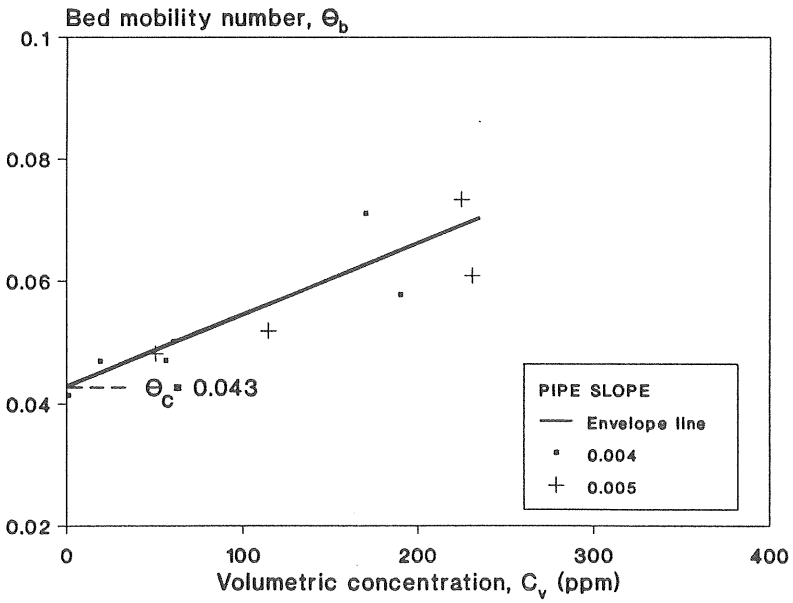

Fig. 5.14 Critical mobility number for sand size D_{50} = 2.5 mm

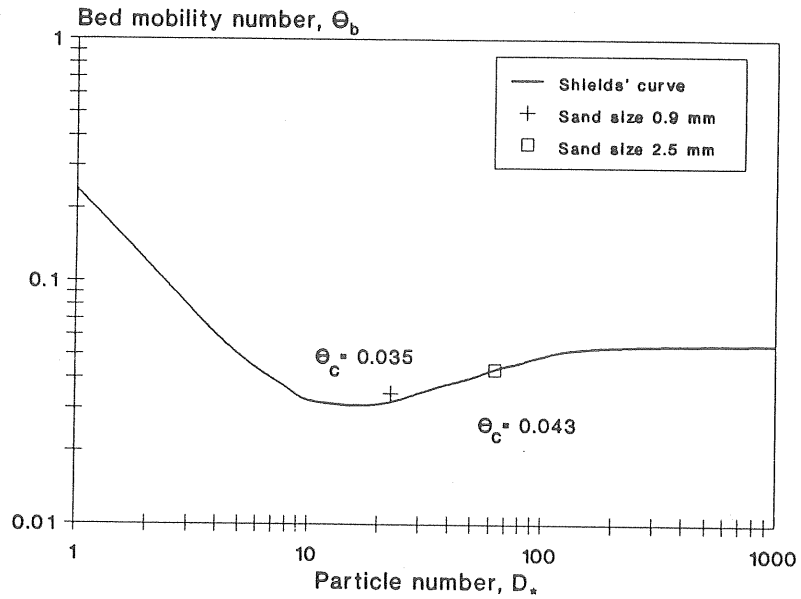

Fig. 5.15 Measured critical mobility number plotted in Shields' diagram

5.4 Total bed resistance

Total flow resistance (grain resistance plus form resistance) was predicted using the methods of Engelund-Hansen (1972) and van Rijn (1982) as described in 2.3.1 and was compared with the experimental values calculated directly from the measurements using Eq. (2.13). The bed mobility number, Θ_b, was selected as the common parameter for the comparison. The results are shown in Fig. 5.16 (page 52), from which it can be seen that both methods have a certain degree of agreement with the measured values. As both methods were designed for wide alluvial channels (no side wall correction required), a perfect agreement cannot be expected.

Engelund and Hansen (1972) presented a relationship between the bed mobility number, Θ_b, and the grain mobility number, Θ_b', for dunes in alluvial channels while Lau (1988) suggested one for ripples, based on flume experiments and field data also from alluvial channels. Thus, it is desirable to establish a relationship for pipe channels with a deposited bed.

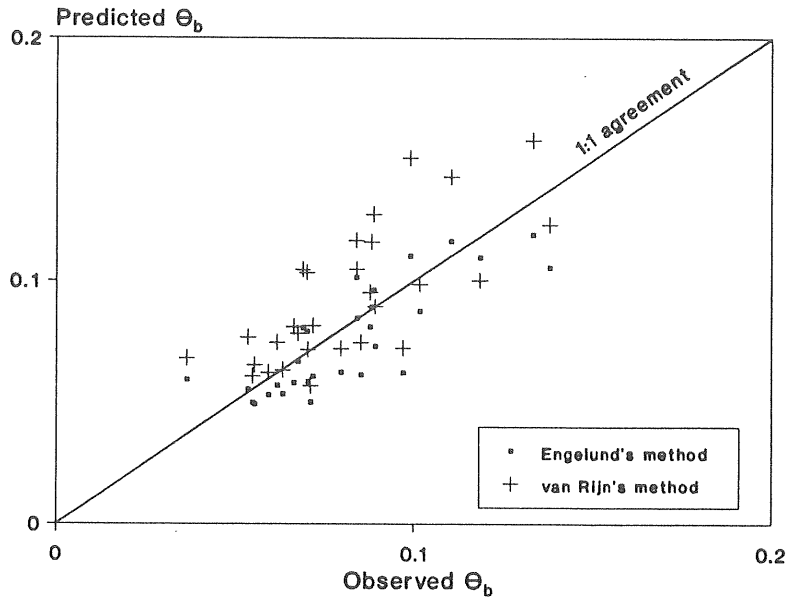

Fig. 5.16 Predicted vs. observed total bed flow resistance

The present study differs from the above in that some bedforms were identified in the transitional regime while the majority were definitely in the hydraulically rough regime. This fact has not only been observed in the laboratory but also in the field (Lyngfelt 1990) which suggests that this may be the general case for stream traction in pipe channels.

A similar approach to those mentioned above was done for the present measurements. The dimensionless ratios Θ_b/Θ_c versus Θ_b'/Θ_c were plotted and the results are shown in Fig. 5.17. The value of Θ_b' was calculated using Eq. (2.15). The grain shear velocity was determined from Eqs. (2.4) and (2.5) using R_b from the side wall elimination procedure and $k_b' = 2.5\ D_{50}$ which is appropriate for the sand sizes of the present experimental study.

The results from previous experiments (Perrusquía 1990A) and from the two complementary series carried out in England (Perrusquía 1990B) were also included.

The data show the effect of bedforms on the total resistance. All measurements were included in Fig. 5.17, even those where the sediment bed is almost plane,

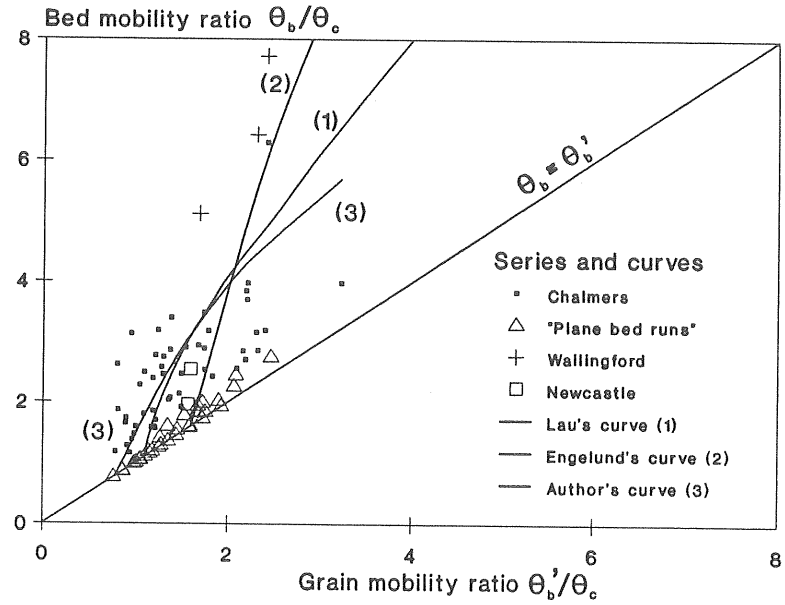

Fig. 5.17 Θ_b/Θ_c vs. Θ_b'/Θ_c for present experimental data

i.e. ($\Theta_b \equiv \Theta_b'$). The points of interest in this case are from the runs that developed bedforms which show similar tendencies to those of the data of Lau (1988) and Engelund-Hansen (1972), whose proposed curves are also included in Fig. 5.17. The best-fit curve for the present measurements is:

$$\Theta_b/\Theta_c = 1.5 + 3.58 \text{ Ln } (\Theta_b'/\Theta_c) \qquad (5.1)$$

The upper limit could not be defined since the range of the experiments did not cover the flow regime at which the bedforms eventually disappear. However, Eq. (5.1) can be used in a design method for the conditions of the present study. The computational procedure consists of several equations which can be solved iteratively as follows:

1) Knowing: Flow discharge, Q
Water density, ρ
Side wall roughness, k_w
Pipe slope, S
Sand size, D_{50}, and density, ρ_s
Sediment bed thickness, t

2) Assume a value for the flow depth, Y.

3) Determine the hydraulic radius of the bed, R_b, using the side wall elimination procedure.

4) Calculate the bed mobility number, Θ_b, using Eq. (2.13)

$$\Theta_b = \frac{R_b\ S}{(s-1)D_{50}} \qquad (2.13)$$

5) Estimate the grain mobility number, Θ_b', using Eq. (5.1) or the curve from Fig. 5.17.

6) Calculate the shear velocity, u_*, using Eq. (2.15)

$$\Theta_b' = \frac{(u_*')^2}{(s-1)_g\ D_{50}} \qquad (2.15)$$

7) Calculate the mean flow velocity, V, using an expression similar to Eqs. (2.4) or (2.5) but applied to the shear velocity corresponding to the grain, i.e.

$$\frac{V}{u_*} = 5.75 \log \left[12 \frac{R_b}{k_b}\right] \qquad (2.5)$$

6) Calculate the flow discharge, Q = V A and compare it with the known discharge. The process is repeated from step (2) until an acceptable difference is achieved.

5.5 Bedform height and length

The proposal of a method for the prediction of bedform dimensions is beyond the scope of this thesis. The methods of Fredsoe (1982) and van Rijn (1984) as described in 2.3.2 were used for the prediction of bedform height and length. The predictors were compared with the measured bedforms and the results are shown in Figs. 5.18 and 5.19 (page 56).

The method of Fredsoe gives reasonable bedform height predictions. On the other hand, it underestimates bedform length even though Eq. (2.30) was used which relates bedform length not only to bedform height but also to both the mobility number, Θ_b, and the critical mobility number, Θ_c. This may be due to the fact that the curve that Fredsoe (1982) presented, which is based on a differential equation whose approximation is given by Eq. (2.30), was drawn for a particular value of the critical mobility number, Θ_c. The implementation of new curves for different values of Θ_c may lead to better bedform length predictions. Work is currently being done in that direction (Mark 1991).

The method of van Rijn overestimates both height and length. One of the reasons for this outcome is that Eq. (2.30) is very sensitive to the value of the transport stage parameter, T, which in turn is a function of the grain mobility number, Θ_b', according to Eq. (2.32). Following van Rijn's method, Θ_b' was computed using a value for the equivalent sand roughness, $k_b' = 3\ D_{90}$. This made Θ_b' adopt values which in some cases exceeded the value of the bed mobility number, Θ_b , which is physically impossible. By using 2.5 D_{50} instead of 3 D_{90}, a better agreement is achieved. The former is a better estimate of k_b' for the sand size used in the present study (Engelund and Hansen 1972, van Rijn 1988). van Rijn related bedform length exclusively to flow depth ($L \cong 7.3\ Y$) which gives lengths up to twice the size of the measured values.

Similar to what is discussed in the previous section, these two methods are applicable to wide alluvial channels and there may be other parameters affecting the development of bedforms in pipe channels which are not considered by either of these methods. Moreover, the range of the present experimental data may not lie completely within the range of application of both methods.

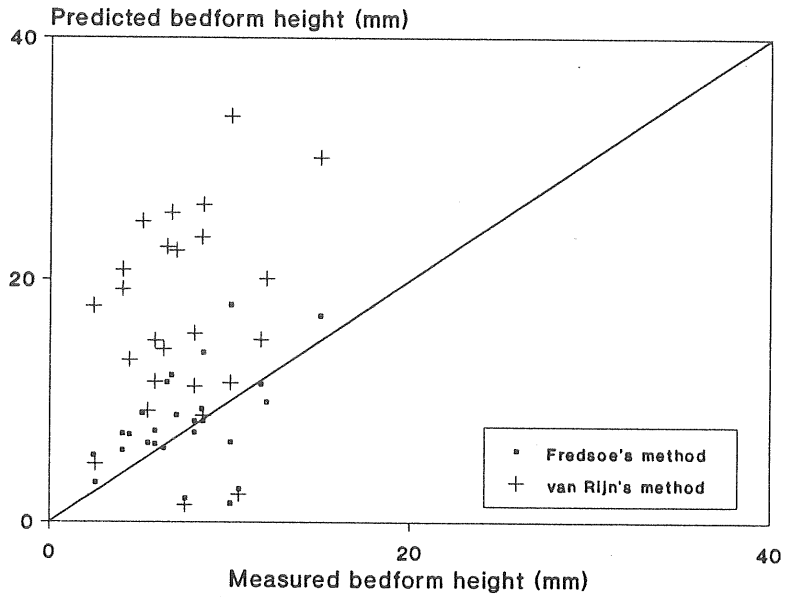

Fig. 5.18 Comparison between predicted and observed bedform height

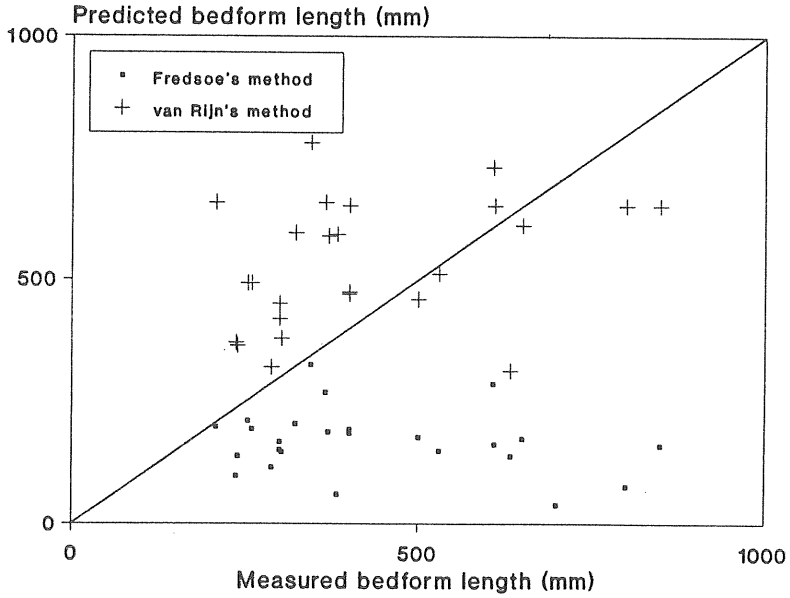

Fig. 5.19 Comparison between predicted and observed bedform length

5.6 Bedload transport equation

5.6.1 Individual analysis

All three series, Chalmers, Wallingford and Newcastle, were used. Each of the dimensionless parameters presented in Chapter 3 were plotted against the transport parameter to detect any indication of dependance. The effect that shear stress has on sediment transport is illustrated in Fig. 5.20 (page 58) where the observed values for the transport parameter, Φ_b, are plotted against the bed mobility number, Θ_b. It is clear that shear stress plays an important role in the motion of particles and some of the most commonly used equations express sediment transport as a function of shear stress exclusively.

Bed mobility number, Θ_b, seems to be sufficient to describe the sediment transport process. However, the significance of the other parameters involved in the functional relationship expressed in Eqs. (3.1) and (3.10) was investigated.

The particle number, D_*, does not appear to have a great influence on transport if only a few values of D_* are available. A different tendency is noticeable if one looks at the whole range of particle numbers. Ackers and White (1973) and van Rijn (1984) did similar analyses for wider ranges of particle sizes and in both studies the influence of D_* on transport is clearly shown.

The small variations in sand density, ρ_s, make the relative density, s, by itself, rather irrelevant. Further, s is only important when dealing with individual particles (Yalin 1972). None of the parameters, relative wall roughness, D_{50}/k_w, relative bed thickness, t/D, or relative total depth, (Y+t)/D, show any apparent influence on transport.

The relative grain size, $Z = D_{50}/Y$, has a more definite effect on transport as shown in Fig. 5.21 (page 59). The same applies to the relative flow depth, Y/D, which is shown in Fig. 5.22 (page 59). In a study by May et al (1989), Y/D was found relevant in the structure of the equation to define the limit of deposition of particles in flume traction with a deposited bed of 0.01 D.

Nevertheless, all of the aforementioned parameters are incorporated in the next stage of the analysis because it is the author's belief that the influence of the geometric parameters is of some significance when they are used in combination with the other dimensionless parameters.

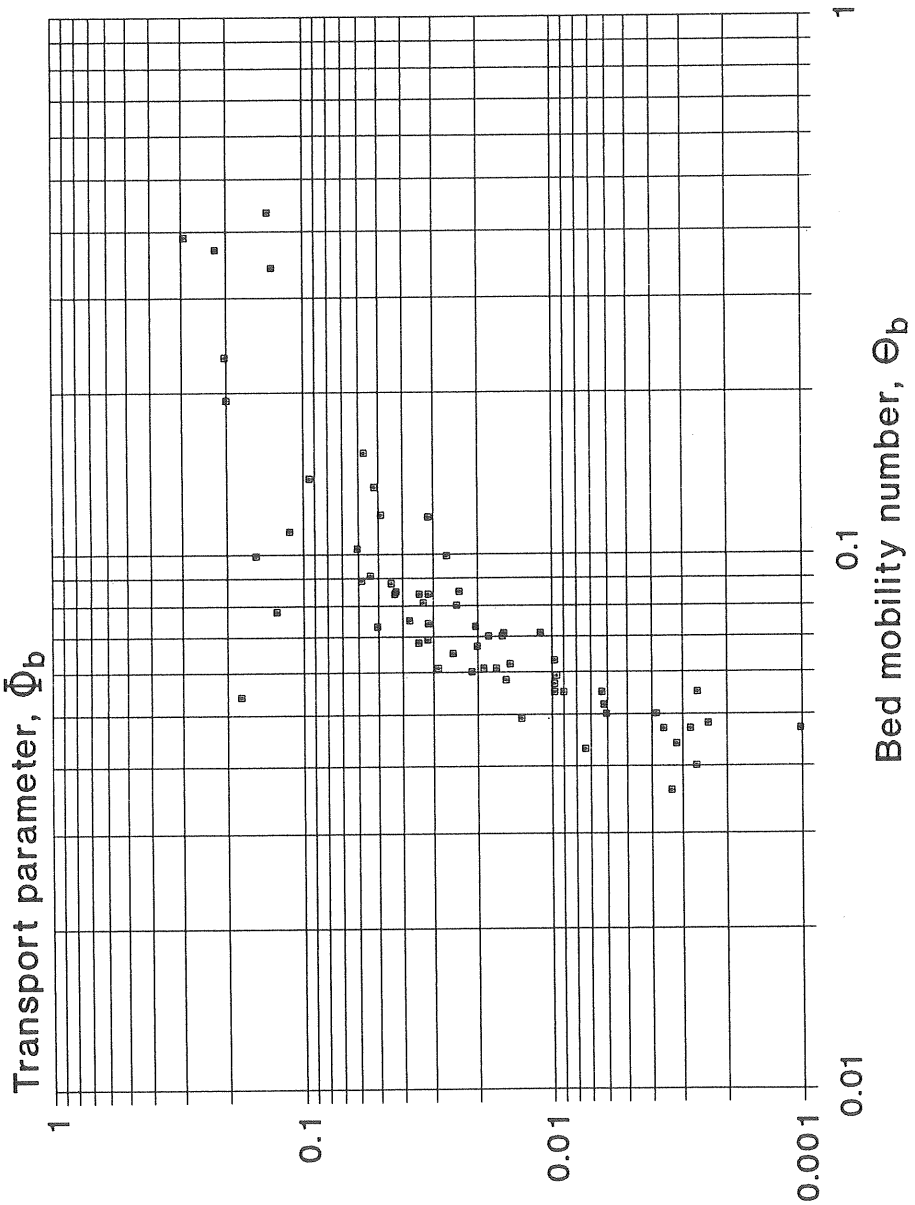

Fig. 5.20 Transport parameter versus bed mobility number

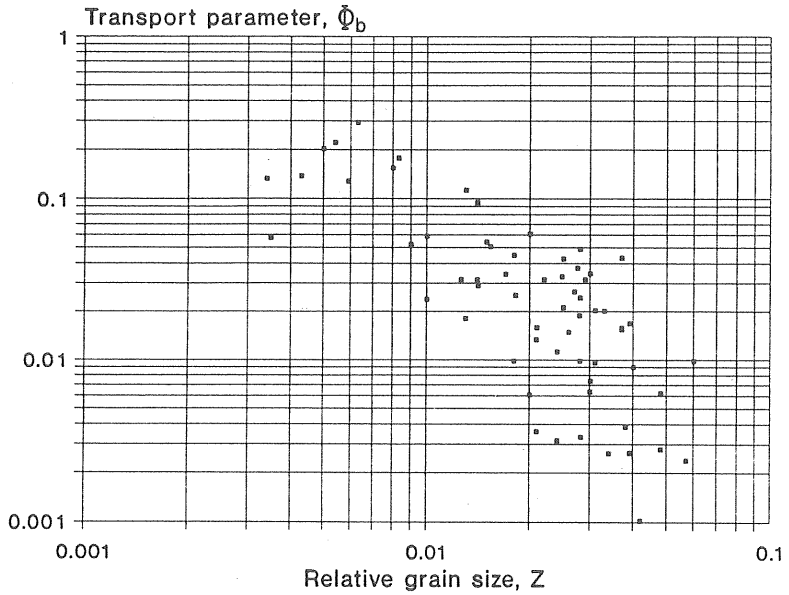

Fig. 5.21 Transport parameter versus relative grain size

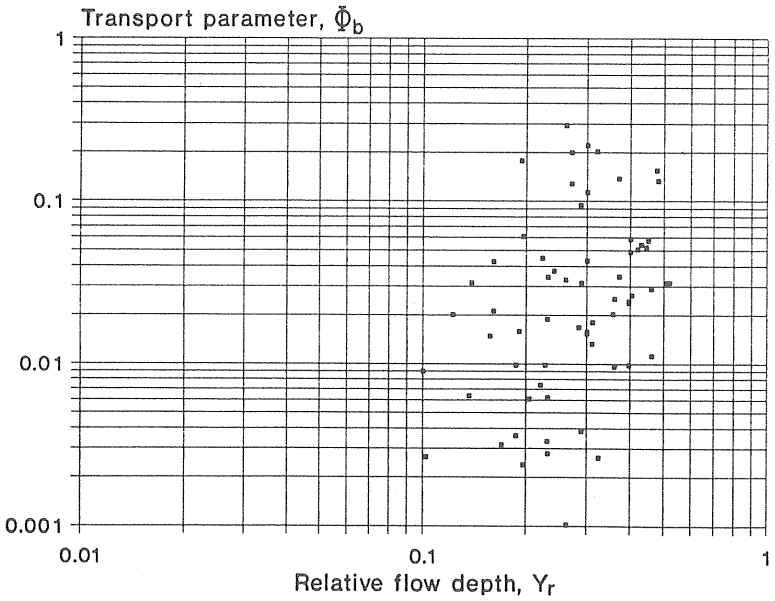

Fig. 5.22 Transport parameter versus relative flow depth

5.6.2 Simultaneous analysis

To study the dependence of transport on all the aforementioned dimensionless parameters, multiple regression analysis was used. Linear least squares regression, with the dimensionless parameters as independent variables, was performed to find the regression model. The STATGRAPHICS System was used for the computations. All three series, Chalmers, Wallingford and Newcastle, were used. A total of 49 regression and analysis of variance tests were executed. The analysis was carried out considering all the dimensionless variables of the functional relationship as expressed in Eq. (3.1) which is re-written below

$$\Phi_b = f_1(\Theta_b, D_*, s, Z, Y_r, t_r, k_r) \qquad (3.1)$$

The significance of two variables, namely s and k_r was found to be almost negligible. This was expected since they did not show a great influence on transport in the individual analysis. They were excluded from the subsequent analysis to find the model that fits the experimental data. Of the remaining five parameters, Z did not show a significant contribution to the fit. The equation which contains the parameters that describe sediment transport for the present conditions has the form

$$\Phi_b = 4.56\ \Theta_b^{1.23}\ D_*^{-0.75}\ Y_r^{0.48}\ t_r^{-0.81} \qquad (5.2)$$

The value of the adjusted coefficient of determination was 0.75. In Fig. 5.23, the comparison between the experimentally determined and the analytically calculated transport parameters shows a rather good agreement. The geometric dimensionless parameters, Y_r and t_r contributed to the inclusion of shape effects in Eq. (5.2).

The equations of Novak and Nalluri (1975), Einstein and Brown (Brown 1950), Meyer-Peter and Müller (1948), Engelund and Fredsøe (1976) and van Rijn (1982) were used to predict the sediment transport parameter using the experimental data and their results were compared with those of the proposed equation. Fig. 5.23 was converted into Fig. 5.24 (page 62) for comparison purposes. Seventy percent of the predicted transport values using Eq. (5.2), which are plotted in Fig. 5.24, are within the ± 50% deviation of the observed values. The outcome from the other equations is presented in Figs. 5.25 to 5.29 (pages 62-64). The first two equations, which are based exclusively on the bed mobility number, Θ_b, gave better results than the remaining three equations, which are based on the excess shear, $(\Theta_b'-\Theta_c)$.

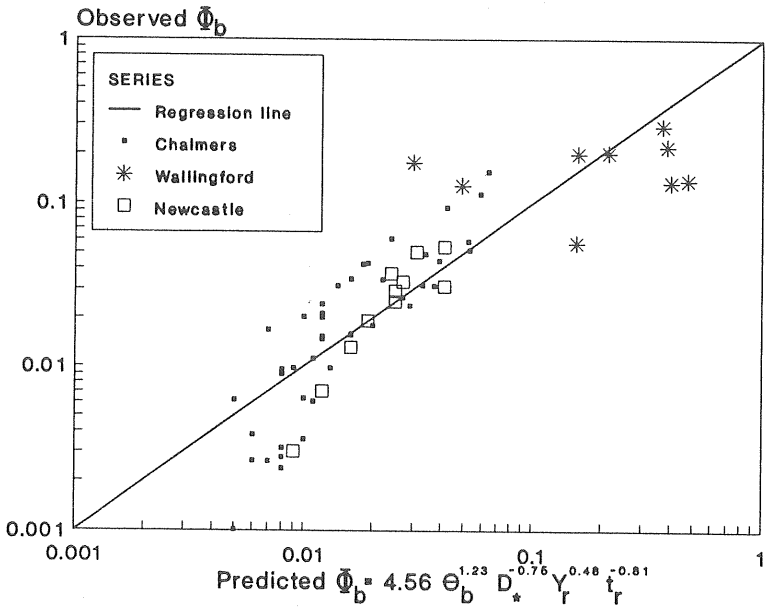

Fig. 5.23 Observed vs. predicted sediment transport using Eq. (5.2)

The significance of another parameter was also tested, namely the relative total depth, (Y+t)/D, to identify the influence of the shape of the hydraulic section. This was divided into trapezoidal, (Y+t) ≤ D/2, and concave, (Y+t) > D/2. The functional relationship represented by Eq. (3.10) was used and the same analysis as in the previous case was performed. Similar results were found regarding the significance of the variables s, Z and k_r. The corresponding equation has the form

$$\Phi_b = 15.2\ \Theta_b^{1.27}\ D_*^{-0.77}\ Y_r^{1.14}\ [(Y+t)/D]^{-1.52} \qquad (5.3)$$

Neither a considerable improvement in the fit nor a noticeable pattern for trapezoi dal or concave sections were detected, as shown in Fig. 5.30 (page 65). Therefore, Eq. (5.3) should be seen only as an illustration rather than as an alternative.

From Figs. 5.23 and 5.30, it can be seen that the Wallingford series shows a differ ent tendency from that of the other two series. This is obviously reflected in Figs. 5.24 to 5.29. If the Wallingford series is removed, a considerable improvement in the agreement between observed and predicted transport values can be observed. The points show a more definite tendency to follow a single line, especially for the methods of Novak & Nalluri, Einstein & Brown and Meyer-Peter & Müller.

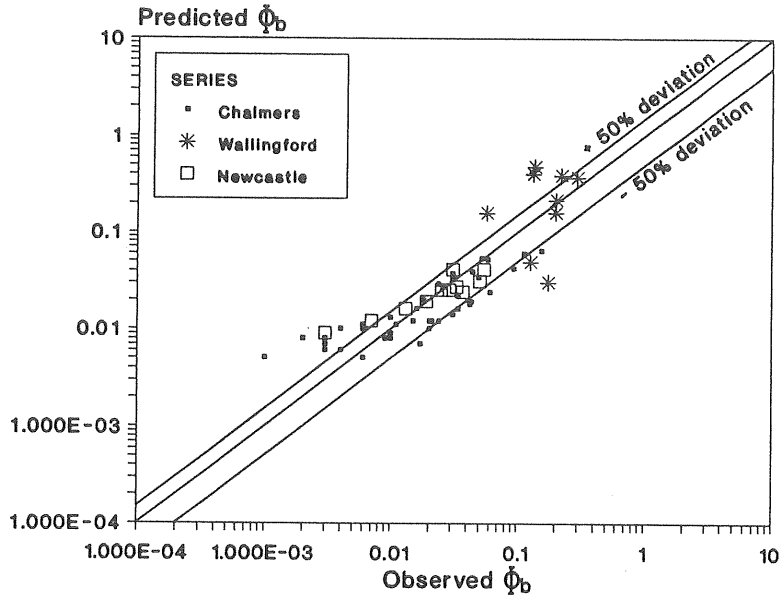

Fig. 5.24 Predicted versus observed transport (Author's equation 5.2)

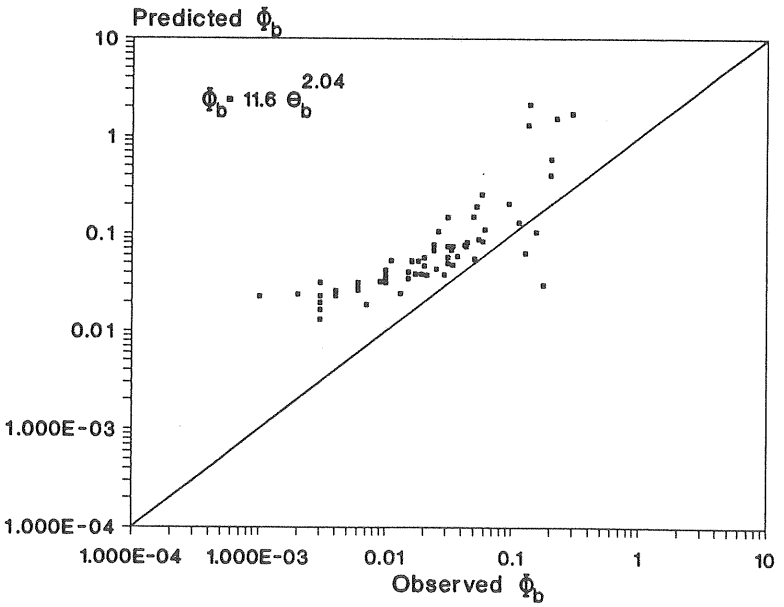

Fig. 5.25 Predicted versus observed transport (Novak-Nalluri's equation)

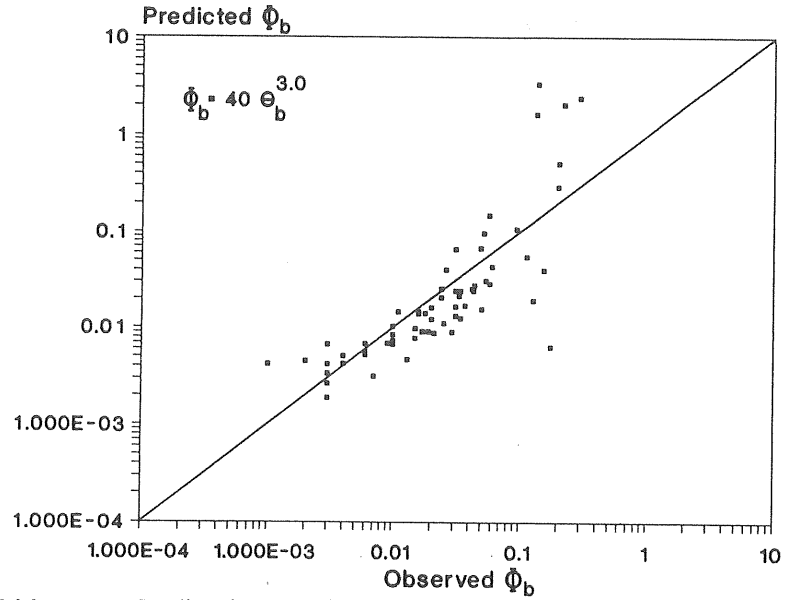

Fig. 5.26 Predicted versus observed transport (Einstein-Brown's equation)

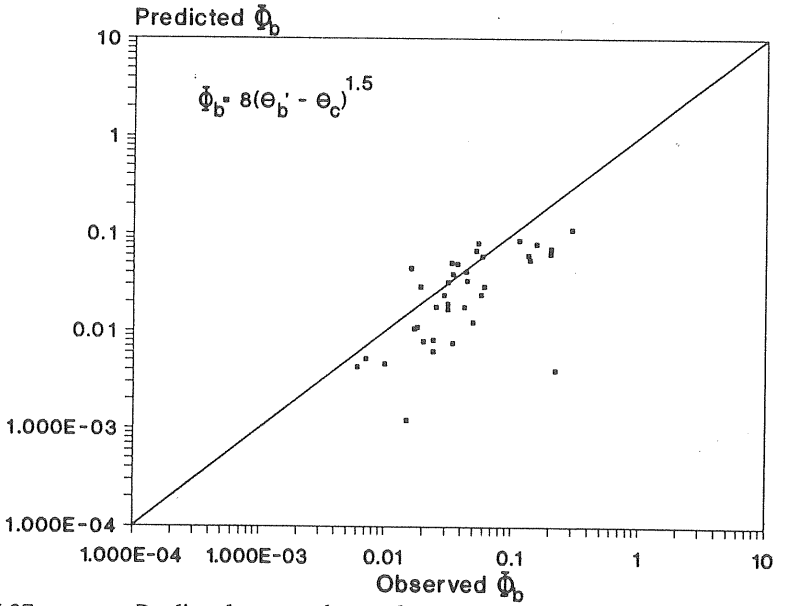

Fig. 5.27 Predicted versus observed transport (Meyer-Peter & Müller's equation)

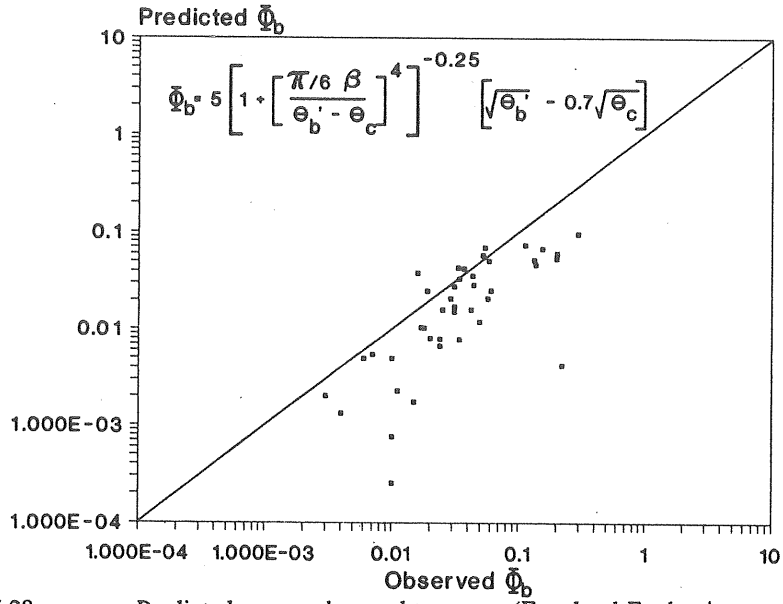

Fig. 5.28 Predicted versus observed transport (Engelund-Fredsøe's equation)

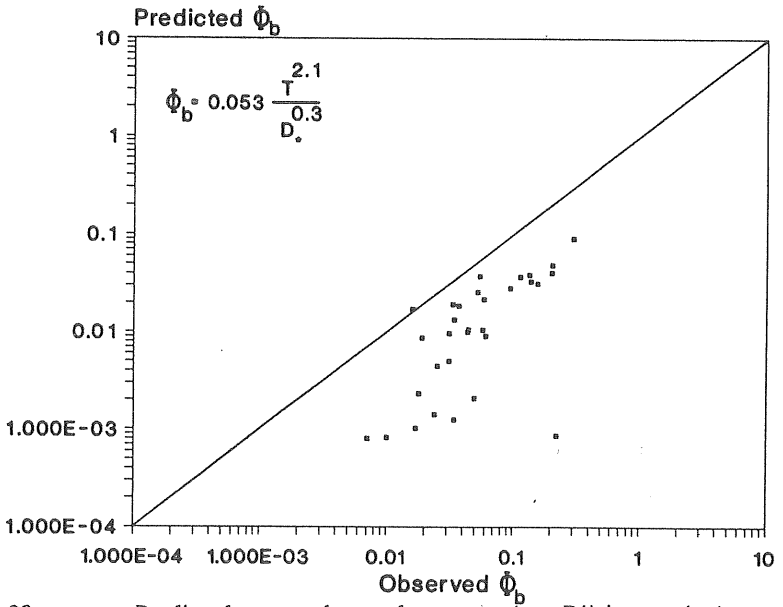

Fig. 5.29 Predicted versus observed transport (van Rijn's equation)

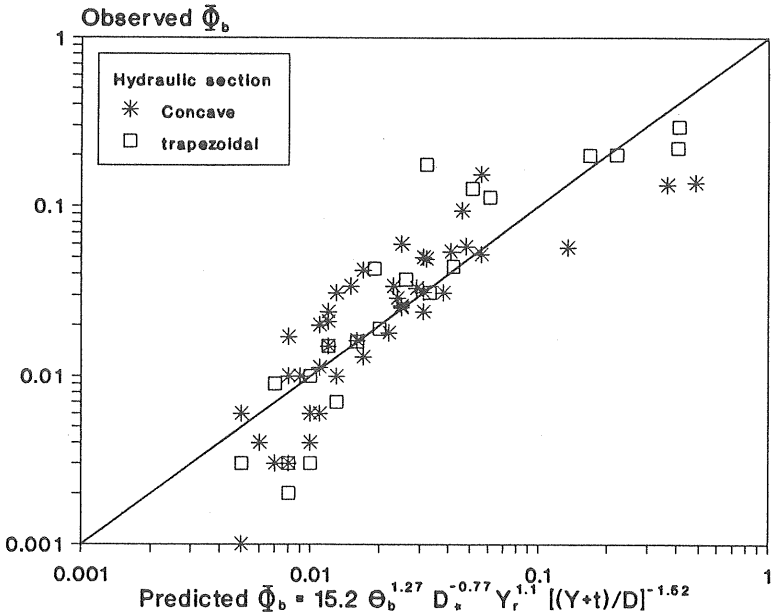

Fig. 5.30 Observed vs. predicted transport using the relative total depth

Sediment transport supply in the Wallingford series was made using a different technique from that used in the other two series. The sediment was not supplied by a feeder but recirculated by a slurry pump. It is possible that the so called "equilibrium condition" had not been achieved by the time transport rates were recorded. Further, the experimental range was very limited which resulted in small variations in parameters such as transport or mobility number. Therefore, it is rather difficult to predict whether the tendency of this series is to follow the regression line before more experiments are made with increased transport rates for this particular pipe diameter (D = 450 mm). It was decided to exclude the Wallingford series from subsequent transport analyses.

Only the data from the Chalmers series and the Newcastle series will be treated henceforth. A total of 49 regression and analysis of variance tests were executed. The proposed equation for the prediction of bedload transport in pipe channels with a deposited sediment bed is

$$\Phi_b = 46137\ \Theta_b^{2.9}\ D_*^{-1.2}\ Z^{0.7}\ Y_r^{0.7}\ t_r^{-0.62} \qquad (5.4)$$

It should be noticed that the parameter Z is included in Eq. (5.4) since it proved to be more significant for the regression model than in the previous analysis. The value of the adjusted coefficient of determination was 0.85, which gives an idea of the improvement in the prediction of sediment transport rates. This is illustrated in Fig. 5.31 where almost ninety percent of the predictions are within ± 50% of the observed values.

The corresponding equation for the relative total depth, (Y+t)/D, is

$$\Phi_b = 86370\ \Theta_b^{2.95}\ D_*^{-1.17}\ Z^{0.66}\ Y_r^{1.15}\ [(Y+t)/D]^{-1.11} \qquad (5.5)$$

Further analyses were made to find the relationship between the transport parameter, Φ_b, and other parameters such as the bed mobility number, Θ_b, and the excess shear, $(\Theta_b' - \Theta_c)$. The aim was to compare the new relationships with the equations suggested by Novak and Nalluri, Einstein and Brown (both based on mobility number) and Meyer-Peter and Müller (based on excess shear). The results are listed in Table 5.5

Table 5.5 Analogous transport equations.

Equations based on mobility number			
Novak-Nalluri (1975) flume traction	Einstein-Brown (1950) alluvial channel	Author stream traction pipe channel	
$\Phi_b = 11.6\ \Theta_b^{2.04}$	$\Phi_b = 40\ \Theta_b^{3.0}$	$\Phi_b = 60\ \Theta_b^{3.05}$	(5.6)
Equations based on excess shear			
Meyer-Peter & Müller (1948) alluvial channel		Author stream traction pipe channel	
$\Phi_b = 8(\Theta_b' - \Theta_c)^{1.5}$		$\Phi_b = 0.6(\Theta_b' - \Theta_c)^{0.75}$	(5.7)

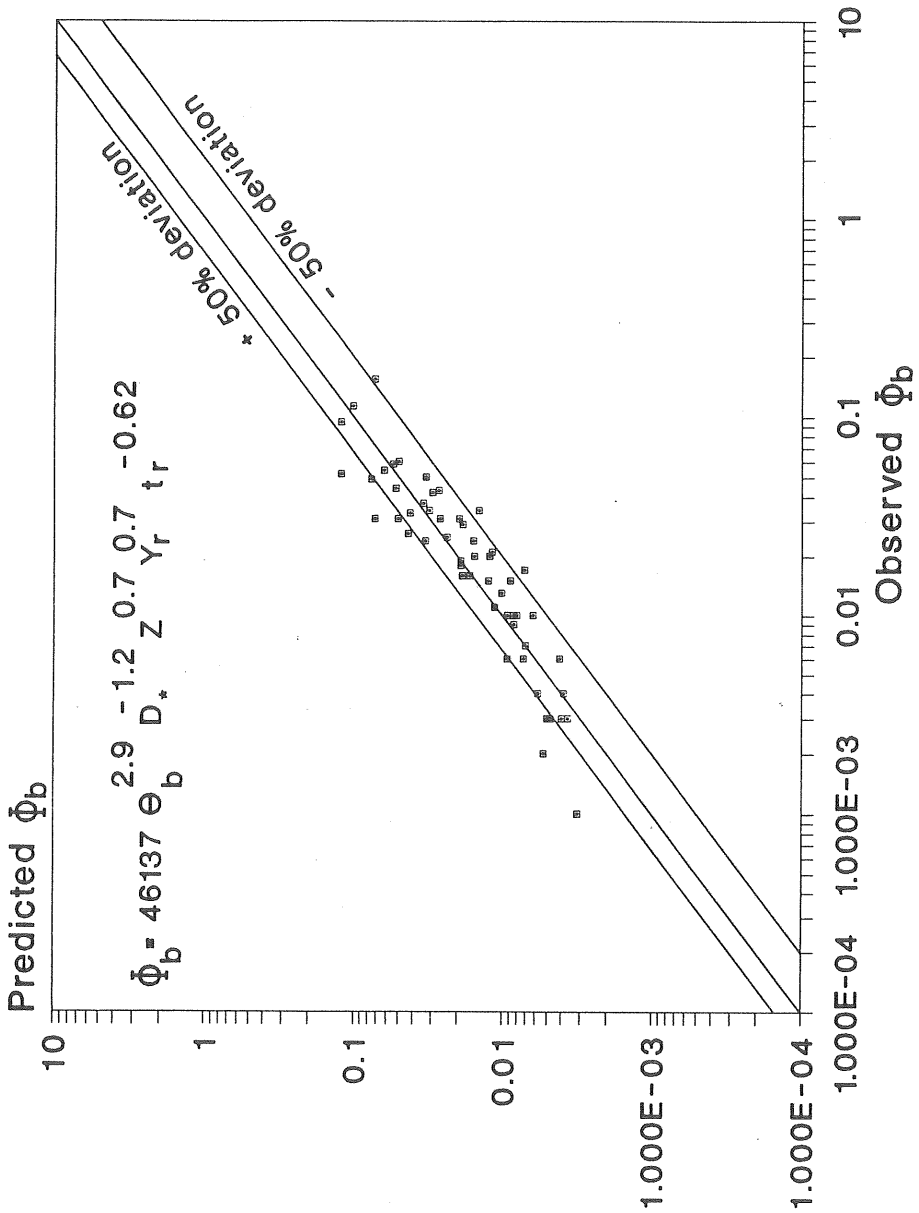

Fig. 5.31 Predicted vs. observed sediment transport using Eq. (5.4)

The value of the adjusted coefficient of determination for Eqs. (5.6) and (5.7) was 0.73 and 0.53, respectively. Figs. 5.32 and 5.33 show plots between observed and predicted transport parameters where it can be seen that fairly good agreement can be obtained by relating transport to one significant parameter. However, Eqs. (5.6) and (5.7), which are adaptations of the original equations listed in Table 5.5 (page 66), should only be seen as a rough estimate of sediment transport in pipe channels. The proposed relationship, Eq. (5.4), gives the best estimate.

A final attempt was made to correlate transport to yet another parameter, namely the total excess shear, $(\Theta_b - \Theta_c)$, which differs from the excess shear of Eq. (5.7) in that the bed mobility number, Θ_b, is included instead of the grain mobility number, Θ_b'. The idea behind this was to assume that the turbulence produced by bedforms results in transport. Therefore, the totality of the shear can be taken as responsible for the sediment transport. Similar analyses were performed and two analogous relationships to Eqs. (5.4) and (5.5) are presented below:

$$\Phi_b = 7.7\,(\Theta_b - \Theta_c)^{0.94}\, D_*^{-0.6}\, Z^{0.24}\, Y_r^{0.46}\, t_r^{-0.82} \qquad (5.8)$$

and

$$\Phi_b = 12.4\,(\Theta_b - \Theta_c)^{0.96}\, D_*^{-0.54}\, Z^{0.16}\, Y_r^{1.04}\, [(Y+t)/D]^{-1.58} \qquad (5.9)$$

The adjusted coefficient of determination was 0.85 for both Eqs. (5.8) and (5.9). Their corresponding plots of the observed against the predicted transport parameters are shown in Figs. 5.34 and 5.35 (page 70).

The above analysis demonstrates how close the different criteria for prediction of sediment transport are. The big difference lies in the applicability of the method and in the selection of the variables that are representative for a particular case.

In summary, Eq. (5.4) is considered to give good estimates of sediment transport in pipe channels. A few considerations should be made:

1) The equation is applicable to the experimental range corresponding to both the Chalmers and Newcastle series.
2) The equation represents a first attempt to compute bedload transport in storm sewers. The difference between the observed and the predicted values of the transport parameter (Φ_b) is acceptable.
3) The equation should be tested for other conditions, i.e. larger pipe diameters and different levels of sediment as well as mixed gradings.

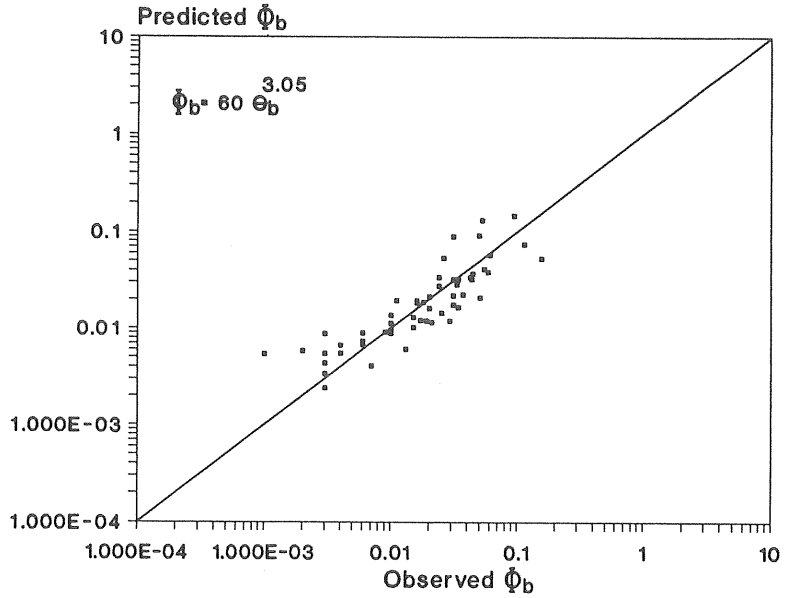

Fig. 5.32 Predicted versus observed transport using Eq. (5.6)

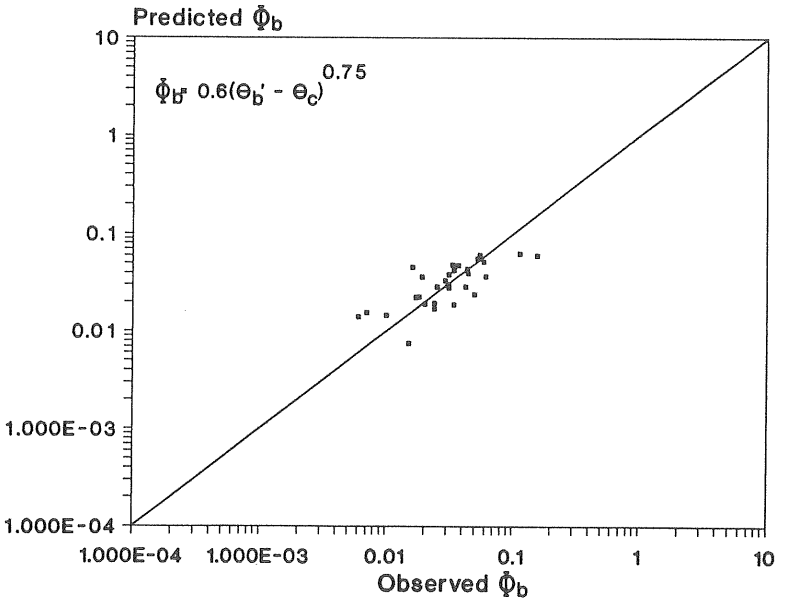

Fig. 5.33 Predicted versus observed transport using Eq. (5.7)

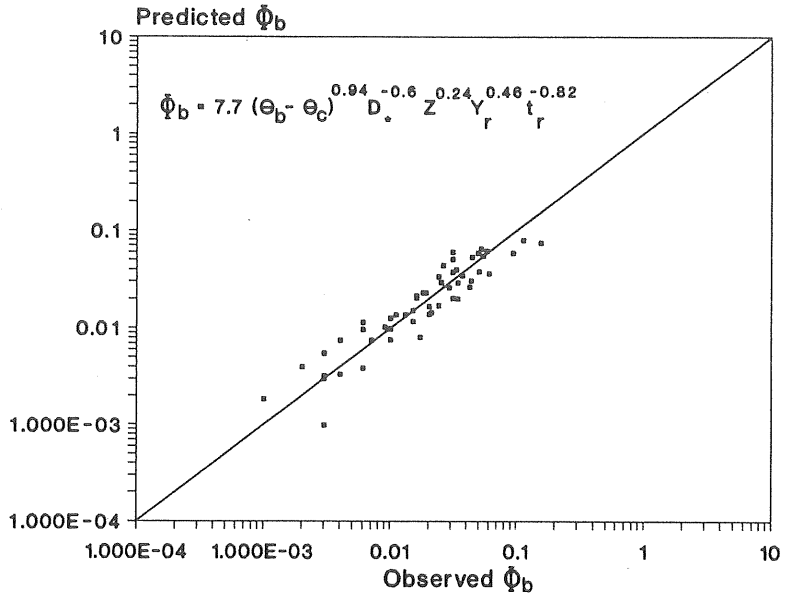

Fig. 5.34 Predicted versus observed transport using Eq. (5.8)

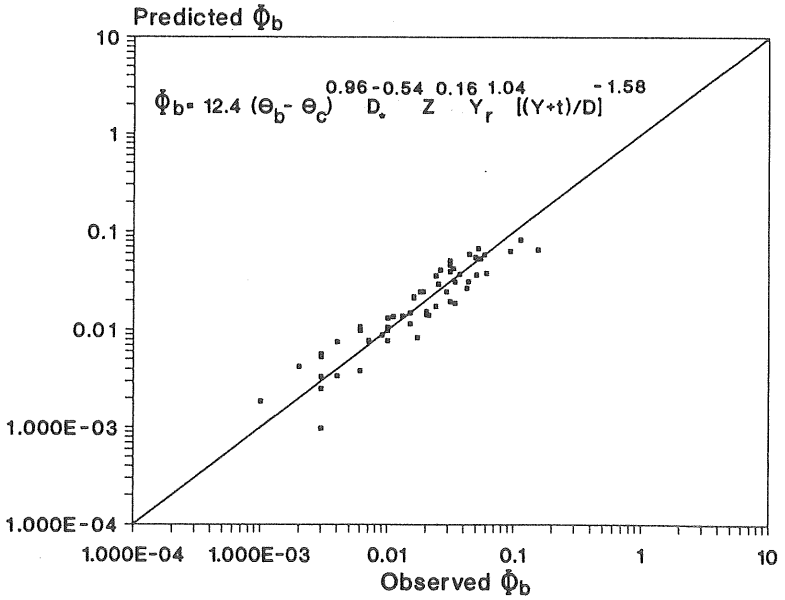

Fig. 5.35 Predicted versus observed transport using Eq. (5.9)

6 FINAL DISCUSSION

6.1 Recapitulation

An experimental study conducted at Chalmers University of Technology has been reported in which the hydraulics of sediment transport in part-full pipes was investigated. The sediment bed was permanently deposited (not fixed) and the type of transport observed and measured was bedload transport exclusively. All these features are included in the sub-title of this thesis: "Stream Traction in Pipe Channels".

The experiments were performed in a concrete pipe which was 225 mm in diameter and 23 m long. Two sand sizes (D_{50}) 0.9 mm and 2.5 mm, were used. Two sediment bed thicknesses were tested, namely 0.2 D and 0.4 D (D being the pipe diameter). Pipe slopes ranged from 0.002 to 0.006.

Two complementary series of experiments were conducted in England. Different pipe diameters, sediment sizes and sediment bed thicknesses were tested. Also, the results from previous experiments were incorporated in the analysis. This additional information allowed the present study a wider range of application: 154 mm to 225 mm, for pipe diameter and 0.5 mm to 2.5 mm, for sand size. A total of 78 independent runs were carried out of which 58 are reported in this thesis. The remaining 20 runs have been already reported by the author in a previous publication (Perrusquía 1990B).

The experiments were run under uniform flow conditions. Flow depths, flow discharge rates, flow velocitites, sediment supply rates, sediment transport rates, bedform dimensions and shear stresses were measured. The reproducibility of the runs was tested in a few cases and was found satisfactory.

6.2 Conclusions

The flow conditions that characterize the stream traction in pipe channels were analyzed and their relationship to flow resistance, bedform dimensions and sediment transport rate was investigated. Three procedures commonly used in this kind of experimental study were tested to corroborate the validity of the computations.

The main conclusions can be listed as follows:

Procedures

- It can be assumed that the vertical velocity distribution near the sediment bed follows a logarithmic law known as the **velocity-defect law**.
- The side wall elimination procedures of Einstein and Vanoni-Brooks can be used to compute the hydraulic radius of the sediment bed with an accuracy which is acceptable for engineering purposes.
- The critical shear stress of the sediment particles can be obtained by using Shields' diagram with good approximation.

Flow resistance

- The methods of Engelund-Hansen and van Rijn for the prediction of flow resistance in alluvial channels were used to compare their predicted values with the experimental data. Both methods have a certain degree of agreement with the measured values bearing in mind that both were designed for wide channels (no side wall correction required).
- The proposed procedure for pipe channels showed similar tendencies to those of the methods of Lau and Engelund-Hansen for ripples and dunes, respectively.

Bedform dimensions

- The methods of Fredsøe and van Rijn for the prediction of bedform geometry in alluvial channels did not give good estimates in the case of pipe channels.

Sediment transport rates

- The proposed equation 5.4 for prediction of bedload transport in pipe channels with a deposited bed fitted fairly well to the experimental data. This equation is expressed in terms of both flow and particle parameters as well as geometric (shape) factors that include both relative flow depth and sediment thickness levels. It has the form

$$\Phi_b = 46137\ \Theta_b^{2.9}\ D_*^{-1.2}\ Z^{0.7}\ Y_r^{0.7}\ t_r^{-0.62}$$

- The equations of Novak and Nalluri and Einstein and Brown, in which transport is exclusively a function of shear stress, gave better estimates than the equations of Meyer-Peter and Müller, Engelund and Fredsøe, and van Rijn, which are based on the excess shear.

Recommendations for future work

1) A proper method for the prediction of bedform geometry which takes into account the geometric characteristics of pipe channels, should be implemented.

2) Both the proposed procedure for the prediction of flow resistance and the proposed equation for bedload transport computation can be used in the analysis of storm sewer systems.

3) Further experimental work with larger pipe diameters, mixed gradings, different levels of sediment and unsteady flow conditions is needed before these methodologies can be fully incorporated in a simulation model.

4) Finally, experimental studies apparently oversimplifly real-world conditions. However, by looking at and understanding one part of the problem at a time, the problem as a whole can be understood and solved.

REFERENCES

Ackers, P. and White, W. (1973): Sediment transport: new approach and analysis. Journal of the Hydraulics Division, ASCE, vol. 99, no. 11, USA.

Allen, J. R. L. (1968): Current Ripples. North Holland Publishing Company, Amsterdam, The Netherlands.

Brown, C. B. (1950): Engineering Hydraulics, H. Rouse (ed), John Wiley and Sons, New York, USA.

Chow, V. T. (1959): Open-Channel Hydraulics. McGraw-Hill Book Company, New York, USA.

Danish Hydraulic Institute (1986): S11TD and ST. Scientific Documentation, Appendix I. Denmark.

Einstein, H. A. (1942): Formulas for the transportation of bed load. Transactions, ASCE, Vol. 107, USA.

Engelund, F. and Fredsøe, J. (1976): A sediment transport model for straight alluvial channels. Nordic Hydrology, Vol. 7, Copenhagen, Denmark.

Engelund, F. and Fredsøe, J, (1982): Hydraulic theory of alluvial rivers. Advances in Hydroscience, Vol. 13, Academic Press, San Diego , USA.

Engelund, F. and Hansen, E. (1972): A monograph on sediment transport. Teknisk Forlag, Copenhagen, Denmark.

Fredsøe, J. (1974): On the development of dunes in erodible channels. Journal of Fluid Mechanics, Vol. 64, No. 3, London, England.

Fredsøe, J. (1979): Unstedy flow in straight alluvial streams: modification of individual dunes. Journal of Fluid Mechanics, Vol. 91, No. 3, London, England.

Fredsøe, J. (1982): Shape and dimensions of stationary dunes in rivers. Journal of the Hydraulics Division, ASCE, Vol. 108, No. 8, USA.

Graf, W. H. (1984): Hydraulics of Sediment Transport. Water Resources Publications, Colorado, USA.

Gyr, A. (1989): Personal communication.

Horton, R. E. (1933): Separate roughness coefficients for channel bottom and sides. Engineering News-Record. Vol. 111, USA.

Lau, Y. L. (1988): Hydraulic resistance of ripples. Journal of Hydraulic Engineering, ASCE, Vol. 114, No. 10, USA.

Lau, Y. L. (1989): Personal communication.

Lyngfelt, S. (1990): Hydraulic properties in sewers with sediment. Proceedings, 5th IAHR International Conference on Urban Storm Drainage, Osaka, Japan.

Mark, O. J. (1991): Personal communication.

May, R. W. P. (1982): Sediment transport in sewers. Report No. IT 222, Hydraulics Research Station, Wallingford, England.

May, R. W. P., Brown, P. M., Hare, G. R. and Jones, K. D. (1989): Self-cleansing conditions for sewers carrying sediment. Report SR 221, Hydraulics Research Limited, Wallingford, England.

Meyer-Peter, E. and Müller, R. (1948): Formulas for bed-load transport. Proceedings, 2nd IAHSR Meeting, Stockholm, Sweden.

Novak, P. and Nalluri, C. (1972): A study into the correlation of sediment motion in pipe and open channel flow. Proceedings, 2nd BHRA International Conference on the Hydraulic Transport of Solids in Pipes, University of Warwick, UK.

Novak, P. and Nalluri, C. (1975): Sediment transport in smooth fixed bed channels. Journal of the Hydraulics Division, ASCE, Vol. 101, No. 9, USA.

Novak, P. and Nalluri, C. (1984): Incipient motion of sediment particles over fixed beds. Journal of Hydraulic Research, IAHR, Vol. 22, No. 3, UK.

Perrusquía, G. (1988): Part-full flow in pipes with a sediment bed. Chalmers University of Technology, Department of Hydraulics, Report Series A:17, Göteborg, Sweden.

Perrusquía, G. (1990A): Flow resistance in storm sewers with a sediment bed. Proceedings, 5th IAHR International Conference on Urban Storm Drainage, Osaka, Japan.

Perrusquía, G. (1990B): Sediment in sewers. Research leaves in England. Chalmers University of Technology, Department of Hydraulics, Report Series B:52, Göteborg, Sweden.

Perrusquía, G., Lyngfelt, S. and Sjöberg, A. (1986): Flödeskapacitet hos avloppsledningar delvis fyllda med sediment. Chalmers University of Technology, Department of Hydraulics, Report Series B:48, Göteborg, Sweden.

Perrusquía, G., Lyngfelt, S. and Sjöberg, A. (1987): Flow capacity of sewers with a sediment bed. Proceedings, 4th IAHR International Conference on Urban Storm Drainage, Lausanne, Switzerland.

Raudkivi, A. J. (1976): Loose Boundary Hydraulics. Pergamon Press, Oxford, England.

Rijn, L. C. van (1982): Equivalent roughness of alluvial bed. Journal of the Hydraulics Division, ASCE, Vol. 108, No. 10, USA.

Rijn, L. C. van (1984A): Sediment transport, Part I: Bed load transport. Journal of Hydraulic Engineering, ASCE, Vol. 110, No. 10, USA.

Rijn, L. C. van (1984B): Sediment transport, Part III: Bedforms and alluvial roughness. Journal of Hydraulic Engineering, ASCE, Vol. 110, No. 12, USA.

Rijn, L. C. van (1988): Personal communication.

Simons, D. B. and Şentürk, F. (1977): Sediment Transport Technology. Water Resources Publications, Colorado, USA.

Vanoni, V. A., Editor (1975): Sedimentation Engineering, ASCE Manual No. 54, New York, USA.

Vanoni, V. A. and Brooks, N. H. (1957): Laboratory studies of the roughness and suspended load of alluvial channels. California Institute of Technology, Report No. E-68, USA

Vanoni, V. A. and Hwang, L. S. (1967): Relation between bed forms and friction in streams. Journal of the Hydraulics Division, ASCE, Vol. 93, No. 3, USA.

Whiting, P. J. and Dietrich, W. E. (1990): Boundary shear stress and roughness over mobile alluvial beds. Journal of Hydraulic Engineering, ASCE, Vol. 116, No. 12, USA.

Yalin, M. S. (1972): Mechanics of Sediment Transport. Pergamon Press, New York, USA.

Yalin, M. S. (1985): On the determination of ripple geometry. Journal of Hydraulic Engineering, ASCE, Vol. 111, No. 8, USA.

APPENDIX

Experimental Data

- All 58 runs of the Chalmers series are listed in pages A.1 to A.5.
- The 44 observations of the Chalmers series listed in pages A.6 and A.7 belong to those runs in which transport rates were measured.
- Eq. (5.2) includes all three series.
- Eqs. (5.4) and (5.9) include only the Chalmers and the Newcastle series.

RUN CHALMERS SERIES	SLOPE	SAND SIZE	SEDIMENT THICKNESS	SEDIMENT WIDTH	FLOW DISCHARGE	FLOW DEPTH
	x 10 E-03	mm	mm	mm	l / s	mm
	S	D_{50}	t	P_b	Q	Y
1	2	0.9	90	220.5	0.49	20
2	2	0.9	90	220.5	1.04	24
3	2	0.9	90	220.5	1.51	30
4	2	0.9	90	220.5	2.00	34
5	2	0.9	90	220.5	2.50	38
6	2	0.9	90	220.5	3.00	42
7	2	0.9	90	220.5	3.50	46
8	2	0.9	90	220.5	4.00	51
9	2	0.9	90	220.5	6.00	70
10	2	0.9	90	220.5	7.50	89
11	3	0.9	90	220.5	0.83	18
12	3	0.9	90	220.5	1.50	26
13	3	0.9	90	220.5	1.75	23
14	3	0.9	90	220.5	2.03	30.5
15	3	0.9	90	220.5	2.50	35
16	3	0.9	90	220.5	3.25	36
17	3	0.9	90	220.5	4.10	43
18	3	0.9	90	220.5	5.00	52
19	3	0.9	90	220.5	10.7	100
20	4	0.9	90	220.5	0.81	15.25
21	4	0.9	90	220.5	1.00	16.5
22	4	0.9	90	220.5	1.50	22.5
23	4	0.9	90	220.5	2.00	27.5
24	4	0.9	90	220.5	2.50	31
25	4	0.9	90	220.5	3.00	36
26	4	0.9	90	220.5	4.00	44
27	4	0.9	90	220.5	7.00	64.5
28	4	2.5	90	220.5	3.00	40
29	4	2.5	90	220.5	4.00	44
30	4	2.5	90	220.5	5.00	51
31	4	2.5	90	220.5	6.00	59
32	4	2.5	90	220.5	7.00	65
33	4	2.5	90	220.5	8.00	73
34	4	2.5	90	220.5	9.00	81
35	4	2.5	90	220.5	10.0	89
36	4	2.5	90	220.5	11.0	104
37	5	2.5	90	220.5	3.00	29
38	5	2.5	90	220.5	4.00	34
39	5	2.5	90	220.5	5.00	49
40	5	2.5	90	220.5	6.0	52
41	5	2.5	90	220.5	8.0	64
42	5	2.5	90	220.5	10.0	80
43	5	2.5	90	220.5	11.0	89
44	5	2.5	45	180.0	4.35	44
45	5	2.5	45	180.0	8.40	67.5
46	5	2.5	45	180.0	11.3	91
47	5	2.5	45	180.0	16.1	115
48	4	2.5	45	180.0	4.50	52
49	4	2.5	45	180.0	7.30	67.5
50	4	2.5	45	180.0	10.5	83.5
51	6	2.5	45	180.0	4.15	42
52	6	2.5	45	180.0	9.50	67.5
53	6	2.5	45	180.0	12.1	90
54	2	0.9	45	180.0	5.95	65
55	2	0.9	45	180.0	9.60	90
56	2	0.9	45	180.0	12.22	107
57	3	0.9	45	180.0	4.37	50
58	3	0.9	45	180.0	7.33	67.5

RUN CHALMERS SERIES	TOTAL DEPTH	RELATIVE TOTAL DEPTH	WATER TEMPERATURE	MEAN TRANSPORT RATE	FLOW VELOCITY	FROUDE NUMBER
	mm		°C	g/min	m/s	
	Y+t	(Y+t)/ D	Tw		V	Fr
1	110	0.49	18		0.110	0.25
2	114	0.51	18		0.194	0.40
3	120	0.53	18		0.225	0.42
4	124	0.55	18		0.263	0.45
5	128	0.57	18	12	0.294	0.48
6	132	0.59	18	13.6	0.319	0.50
7	136	0.60	18	23	0.341	0.50
8	141	0.63	18	37	0.352	0.49
9	160	0.71	18	68	0.390	0.45
10	179	0.80	18	90	0.393	0.39
11	108	0.48	18		0.207	0.49
12	116	0.52	18		0.258	0.51
13	113	0.50	18	10	0.340	0.72
14	120.5	0.54	18	24	0.297	0.54
15	125	0.56	21	56	0.319	0.54
16	126	0.56	18	80	0.403	0.68
17	133	0.59	18	60	0.426	0.65
18	142	0.63	18	130	0.431	0.60
19	190	0.84	18	197	0.510	0.45
20	105.25	0.47	21		0.238	0.62
21	106.5	0.47	22		0.272	0.68
22	112.5	0.50	23	34	0.298	0.64
23	117.5	0.52	20	76	0.325	0.63
24	121	0.54	23	119	0.360	0.65
25	126	0.56	23	161	0.372	0.63
26	134	0.60	22	230	0.407	0.62
27	154.5	0.69	23	357	0.491	0.60
28	130	0.58	21		0.335	0.53
29	134	0.60	20		0.407	0.62
30	141	0.63	20		0.440	0.61
31	149	0.66	23	17.8	0.458	0.59
32	155	0.69	22	67	0.488	0.59
33	163	0.72	23	46	0.500	0.57
34	171	0.76	24	168	0.512	0.54
35	179	0.80	20	171	0.524	0.52
36	194	0.86	20	195	0.509	0.44
37	119	0.53	21		0.462	0.87
38	124	0.55	22		0.526	0.91
39	139	0.62	23		0.457	0.65
40	142	0.63	24	109	0.518	0.72
41	154	0.68	20	294	0.565	0.69
42	170	0.76	20	357	0.575	0.61
43	179	0.80	20	426	0.577	0.57
44	89	0.40	22	34	0.485	0.77
45	112.5	0.50	22	225	0.591	0.75
46	136	0.60	22	380	0.580	0.62
47	160	0.71	22	450	0.655	0.60
48	97	0.43	24	40	0.419	0.61
49	112.5	0.50	23	220	0.513	0.65
50	128.5	0.57	22	492	0.590	0.67
51	87	0.39	22	140	0.486	0.79
52	112.5	0.50	22	616	0.668	0.85
53	135	0.60	20	670	0.629	0.68
54	110	0.49	20	98	0.435	0.56
55	135	0.60	20	181	0.498	0.54
56	152	0.68	20	479	0.533	0.52
57	95	0.42	20	138	0.425	0.63
58	112.5	0.50	20	350	0.515	0.65

RUN CHALMERS SERIES	REYNOLDS NUMBER	HYDRAULIC RADIUS OF THE BED	BED MOBILITY NUMBER	PARTICLE REYNOLDS NUMBER	VOLUMETRIC SEDIMENT CONCENTRAT	TRANSPORT PARAMETER
		m			ppm	
	Re	R_b	Θ_b	Re_*	C_v	Φ_b
1	7091	0.0195	0.0263	16.62		
2	14602	0.0223	0.0300	17.75		
3	20295	0.0272	0.0367	19.63		
4	26133	0.0299	0.0403	20.57		
5	31779	0.0325	0.0437	21.43	30.2	0.00315
6	37122	0.0350	0.0471	22.24	28.5	0.00357
7	42182	0.0374	0.0504	23.01	41.3	0.00604
8	46676	0.0408	0.0550	24.03	58.2	0.00972
9	62230	0.0523	0.0704	27.21	71.3	0.01790
10	69358	0.0633	0.0852	29.92	75.5	0.02360
11	12199	0.0170	0.0343	18.97		
12	20752	0.0238	0.0482	22.49		
13	24756	0.0199	0.0402	20.56	35.9	0.00263
14	27186	0.0273	0.0551	24.06	74.4	0.00630
15	35124	0.0309	0.0623	27.71	141	0.01470
16	41882	0.0297	0.0600	25.11	166	0.02100
17	50398	0.0347	0.0701	27.13	92	0.01580
18	57974	0.0416	0.0840	29.69	166	0.03410
19	92450	0.0659	0.1332	37.41	116	0.05170
20	13172	0.0143	0.0386	21.81		
21	16454	0.0153	0.0412	23.01		
22	24121	0.0206	0.0555	27.34	143	0.00893
23	29010	0.0249	0.0670	28.11	239	0.02000
24	37782	0.0275	0.0740	31.56	299	0.03130
25	43782	0.0317	0.0853	33.89	338	0.04230
26	54046	0.0378	0.1017	36.17	362	0.06040
27	85022	0.0512	0.1379	43.09	323	0.09380
28	40735	0.0359	0.0349	95.90		
29	51776	0.0378	0.0366	96.25		
30	61845	0.0426	0.0413	102.26		
31	75391	0.0483	0.0469	116.32	18.7	0.00101
32	82816	0.0517	0.0501	117.53	60.2	0.00381
33	92275	0.0567	0.0550	126.03	36.2	0.00261
34	101194	0.0613	0.0594	134.01	117	0.00954
35	98025	0.0652	0.0633	126.50	108	0.00972
36	98201	0.0733	0.0711	134.11	112	0.01110
37	43970	0.0248	0.0301	89.10		
38	57831	0.0280	0.0339	96.64		
39	66928	0.0419	0.0508	121.09		
40	80593	0.0427	0.0518	125.05	114	0.00619
41	91228	0.0502	0.0609	124.07	231	0.01670
42	103502	0.0606	0.0734	136.25	225	0.02020
43	107828	0.0658	0.0797	141.98	244	0.02420
44	65466	0.0397	0.0481	115.12	50	0.00236
45	107988	0.0587	0.0711	140.02	170	0.01560
46	126786	0.0819	0.0993	165.41	210	0.02640
47	158972	0.0968	0.1173	179.81	176	0.03130
48	66983	0.0484	0.0470	119.11	56	0.00278
49	96052	0.0595	0.0577	129.11	190	0.01530
50	122840	0.0697	0.0676	136.46	295	0.03420
51	63393	0.0389	0.0565	124.81	212	0.00973
52	122129	0.0577	0.0839	152.08	408	0.04280
53	130778	0.0814	0.1184	173.06	364	0.04860
54	74362	0.0512	0.0690	28.53	104	0.03150
55	103704	0.0658	0.0887	32.35	119	0.05820
56	120520	0.0734	0.0989	34.16	247	0.15400
57	57064	0.0435	0.0878	32.19	199	0.04440
58	85164	0.0547	0.1105	36.12	300	0.11260

RUN CHALMERS SERIES	GRAIN MOBILITY NUMBER	BEDFORM HEIGHT	BEDFORM LENGTH	COMMENTS	COMMENTS	COMMENTS
		mm	mm			
	Θ_b'	H	L			
1				NO TRANSP	PLANE BED	
2				NO TRANSP	PLANE BED	
3				MOVABLE	PLANE BED	
4				MOVABLE	PLANE BED	TRANSP MEAS
5				MOVABLE	PLANE BED	TRANSP MEAS
6				MOVABLE	PLANE BED	TRANSP MEAS
7				MOVABLE	PLANE BED	TRANSP MEAS
8	0.04185	2.5	237	BEDFORMS	PROFILE MEAS	TRANSP MEAS
9	0.04731	5.4	530	BEDFORMS	PROFILE MEAS	TRANSP MEAS
10	0.04504	8.5	610	BEDFORMS	PROFILE MEAS	TRANSP MEAS
11				NO TRANSP	PLANE BED	
12				NO TRANSP	PLANE BED	
13				MOVABLE	PLANE BED	TRANSP MEAS
14				MOVABLE	PLANE BED	TRANSP MEAS
15	0.03782			SMALL BEDFOR		TRANSP MEAS
16				SMALL BEDFOR		TRANSP MEAS
17	0.06612	6.3	633	BEDFORMS	PROFILE MEAS	TRANSP MEAS
18	0.06347	5.8	303	BEDFORMS	PROFILE MEAS	TRANSP MEAS
19	0.07625	15.0	608	BEDFORMS	PROFILE MEAS	
20				MOVABLE	PLANE BED	
21				MOVABLE	PLANE BED	
22				MOVABLE	PLANE BED	TRANSP MEAS
23				MOVABLE	PLANE BED	TRANSP MEAS
24	0.05129			DUNE MOTION		TRANSP MEAS
25	0.05193			DUNE MOTION		TRANSP MEAS
26	0.05843	5.8	288	BEDFORMS	PROFILE MEAS	TRANSP MEAS
27	0.07687	6.4	400	BEDFORMS	PROFILE MEAS	TRANSP MEAS
28				NO TRANSP	PLANE BED	
29				MOVABLE	PLANE BED	
30				MOVABLE	PLANE BED	
31				MOVABLE	PLANE BED	TRANSP MEAS
32	0.04056			DUNE MOTION		TRANSP MEAS
33	0.03905			DUNE MOTION		TRANSP MEAS
34	0.04166	7.5	383	BEDFORMS	PROFILE MEAS	TRANSP MEAS
35	0.04257	10.5	800	BEDFORMS	PROFILE MEAS	TRANSP MEAS
36	0.03837	10.0	700	BEDFORMS	PROFILE MEAS	TRANSP MEAS
37				NO TRANSP	PLANE BED	
38				MOVABLE	PLANE BED	
39				MOVABLE	PLANE BED	
40	0.04955			DUNE MOTION		TRANSP MEAS
41	0.05504			DUNE MOTION		TRANSP MEAS
42	0.05278			DUNE MOTION		TRANSP MEAS
43	0.05143	8.0	850	BEDFORMS	PROFILE MEAS	TRANSP MEAS
44				MOVABLE	PLANE BED	TRANSP MEAS
45				MOVABLE	PLANE BED	TRANSP MEAS
46				MOVABLE	PLANE BED	TRANSP MEAS
47				MOVABLE	PLANE BED	TRANSP MEAS
48				MOVABLE	PLANE BED	TRANSP MEAS
49				MOVABLE	PLANE BED	TRANSP MEAS
50	0.05257	10.0	650	BEDFORMS	PROFILE MEAS	TRANSP MEAS
51				MOVABLE	PLANE BED	TRANSP MEAS
52	0.07266	8.4	260	BEDFORMS	PROFILE MEAS	TRANSP MEAS
53	0.05629	11.7	208	BEDFORMS	PROFILE MEAS	TRANSP MEAS
54	0.06009	8.0	400	BEDFORMS	PROFILE MEAS	TRANSP MEAS
55	0.07274	8.5	366	BEDFORMS	PROFILE MEAS	TRANSP MEAS
56	0.08063	10.0	345	BEDFORMS	PROFILE MEAS	TRANSP MEAS
57	0.06067	4.4	239	BEDFORMS	PROFILE MEAS	TRANSP MEAS
58	0.08326	6.7	254	BEDFORMS	PROFILE MEAS	TRANSP MEAS

OBSERVATION	TRANSPORT PARAMETER	MOBILITY NUMBER	PARTICLE NUMBER	RELATIVE GRAIN SIZE	RELATIVE FLOW DEPTH
	EXPERIMENTAL VALUES	EXPERIMENTAL VALUES	EXPERIMENTAL VALUES	EXPERIMENTAL VALUES	EXPERIMENTAL VALUES
	Φ_b	Θ_b	D_*	$Z = D_{84}/Y$	$Yr = Y/D$
CHALMERS 1	0.003	0.044	21.9	0.024	0.169
2	0.004	0.047	21.9	0.021	0.187
3	0.006	0.050	21.9	0.020	0.204
4	0.010	0.055	21.9	0.018	0.227
5	0.018	0.070	21.9	0.013	0.311
6	0.024	0.085	21.9	0.010	0.396
7	0.003	0.040	21.9	0.039	0.102
8	0.006	0.055	21.9	0.030	0.136
9	0.015	0.062	23.1	0.026	0.156
10	0.021	0.060	21.9	0.025	0.160
11	0.016	0.070	21.9	0.021	0.191
12	0.034	0.084	21.9	0.017	0.231
13	0.052	0.133	21.9	0.009	0.444
14	0.009	0.056	23.8	0.040	0.100
15	0.020	0.067	22.8	0.033	0.122
16	0.031	0.074	23.8	0.029	0.138
17	0.042	0.085	23.8	0.025	0.160
18	0.060	0.102	23.4	0.020	0.196
19	0.094	0.138	23.8	0.014	0.287
20	0.001	0.047	66.1	0.042	0.262
21	0.004	0.050	65.1	0.038	0.289
22	0.003	0.055	66.1	0.034	0.324
23	0.010	0.059	67.1	0.031	0.360
24	0.010	0.063	63.2	0.028	0.396
25	0.011	0.071	63.2	0.024	0.462
26	0.006	0.052	67.1	0.048	0.231
27	0.017	0.061	63.2	0.039	0.284
28	0.020	0.073	63.2	0.031	0.356
29	0.024	0.080	63.2	0.028	0.396
30	0.002	0.048	65.1	0.057	0.196
31	0.016	0.071	65.1	0.037	0.300
32	0.026	0.099	65.1	0.027	0.404
33	0.031	0.117	65.1	0.022	0.511
34	0.003	0.047	67.1	0.048	0.231
35	0.015	0.058	66.1	0.037	0.300
36	0.034	0.068	65.1	0.030	0.371
37	0.010	0.057	65.1	0.060	0.187
38	0.043	0.084	65.1	0.037	0.300
39	0.049	0.118	63.2	0.028	0.400
40	0.032	0.069	22.8	0.014	0.289
41	0.058	0.089	22.8	0.010	0.400
42	0.154	0.099	22.8	0.008	0.476
43	0.044	0.088	22.8	0.018	0.222
44	0.113	0.111	22.8	0.013	0.300
WALLINGF 1	0.176	0.054	16.7	0.008	0.193
2	0.127	0.078	16.4	0.006	0.270
3	0.057	0.154	16.7	0.004	0.450
4	0.199	0.193	16.1	0.001	0.270
5	0.201	0.232	16.1	0.005	0.320
6	0.133	0.341	16.1	0.003	0.480
7	0.220	0.369	16.1	0.005	0.300
8	0.137	0.433	16.1	0.004	0.370
9	0.293	0.389	16.1	0.006	0.260
NEWCASTLE 1	0.007	0.043	24.3	0.030	0.220
2	0.025	0.065	24.3	0.018	0.360
3	0.031	0.084	24.3	0.013	0.520
4	0.019	0.061	24.3	0.028	0.230
5	0.050	0.073	24.3	0.015	0.420
6	0.054	0.091	24.3	0.015	0.430
7	0.033	0.081	25.3	0.025	0.260
8	0.037	0.075	25.3	0.028	0.240
9	0.003	0.036	25.3	0.028	0.230
10	0.029	0.061	25.3	0.014	0.460
11	0.013	0.049	24.3	0.021	0.310

OBSERVATION		RELATIVE BED THICKNESS	RELATIVE DENSITY	RELATIVE TOTAL DEPTH	RATIO SAND SIZE/WALL ROUGHNESS	TRANSPORT PARAMETER PROPOSED EQUATION
		EXPERIMENTAL VALUES	EXPERIMENTAL VALUES	EXPERIMENTAL VALUES	EXPERIMENTAL VALUES	5.2
		$tr = t/D$	s	$(Y+t)/D$	D_{50}/k	Φ_b
CHALMERS	1	0.40	2.65	0.569	6.0	0.008
	2	0.40	2.65	0.587	6.0	0.010
	3	0.40	2.65	0.604	6.0	0.011
	4	0.40	2.65	0.627	6.0	0.013
	5	0.40	2.65	0.711	6.0	0.020
	6	0.40	2.65	0.796	6.0	0.029
	7	0.40	2.65	0.502	6.0	0.006
	8	0.40	2.65	0.536	6.0	0.010
	9	0.40	2.65	0.556	6.0	0.012
	10	0.40	2.65	0.560	6.0	0.012
	11	0.40	2.65	0.591	6.0	0.016
	12	0.40	2.65	0.631	6.0	0.022
	13	0.40	2.65	0.844	6.0	0.053
	14	0.40	2.65	0.500	6.0	0.008
	15	0.40	2.65	0.522	6.0	0.012
	16	0.40	2.65	0.538	6.0	0.014
	17	0.40	2.65	0.560	6.0	0.018
	18	0.40	2.65	0.596	6.0	0.024
	19	0.40	2.65	0.687	6.0	0.042
	20	0.40	2.65	0.662	16.7	0.005
	21	0.40	2.65	0.689	16.7	0.006
	22	0.40	2.65	0.724	16.7	0.007
	23	0.40	2.65	0.760	16.7	0.008
	24	0.40	2.65	0.796	16.7	0.009
	25	0.40	2.65	0.862	16.7	0.011
	26	0.40	2.65	0.631	16.7	0.005
	27	0.40	2.65	0.684	16.7	0.007
	28	0.40	2.65	0.756	16.7	0.010
	29	0.40	2.65	0.796	16.7	0.012
	30	0.20	2.65	0.396	16.7	0.008
	31	0.20	2.65	0.500	16.7	0.016
	32	0.20	2.65	0.604	16.7	0.027
	33	0.20	2.65	0.711	16.7	0.037
	34	0.20	2.65	0.431	16.7	0.008
	35	0.20	2.65	0.500	16.7	0.012
	36	0.20	2.65	0.571	16.7	0.016
	37	0.20	2.65	0.387	16.7	0.009
	38	0.20	2.65	0.500	16.7	0.019
	39	0.20	2.65	0.600	16.7	0.034
	40	0.20	2.65	0.489	6.0	0.033
	41	0.20	2.65	0.600	6.0	0.052
	42	0.20	2.65	0.676	6.0	0.064
	43	0.20	2.65	0.422	6.0	0.039
	44	0.20	2.65	0.500	6.0	0.059
WALLINGF	1	0.16	2.65	0.353	4.8	0.030
	2	0.19	2.65	0.460	4.8	0.049
	3	0.17	2.65	0.620	4.8	0.156
	4	0.18	2.65	0.450	4.8	0.158
	5	0.18	2.65	0.500	4.8	0.215
	6	0.19	2.65	0.670	4.8	0.402
	7	0.17	2.65	0.470	4.8	0.386
	8	0.19	2.65	0.560	4.8	0.476
	9	0.18	2.65	0.440	4.8	0.369
NEWCASTLE	1	0.27	2.59	0.490	15.0	0.012
	2	0.27	2.59	0.630	15.0	0.025
	3	0.27	2.59	0.790	15.0	0.041
	4	0.27	2.59	0.500	15.0	0.019
	5	0.27	2.59	0.690	15.0	0.031
	6	0.27	2.59	0.700	15.0	0.041
	7	0.27	2.59	0.530	15.0	0.027
	8	0.27	2.59	0.510	15.0	0.024
	9	0.27	2.59	0.500	15.0	0.009
	10	0.27	2.59	0.730	15.0	0.025
	11	0.27	2.59	0.580	15.0	0.016

OBSERVATION		PROPOSED EQUATION 5.4 TRANSPORT PARAMETER PREDICTED VALUES MULTIPLE REGRESSION $\bar{\Phi}_b$	PROPOSED EQUATION 5.5 TRANSPORT PARAMETER PREDICTED VALUES MULTIPLE REGRESSION $\bar{\Phi}_b$	PROPOSED EQUATION 5.6 TRANSPORT PARAMETER PREDICTED VALUES MULTIPLE REGRESSION $\bar{\Phi}_b$	PROPOSED EQUATION 5.7 TRANSPORT PARAMETER PREDICTED VALUES MULTIPLE REGRESSION $\bar{\Phi}_b$	PROPOSED EQUATION 5.8 TRANSPORT PARAMETER PREDICTED VALUES MULTIPLE REGRESSION $\bar{\Phi}_b$	PROPOSED EQUATION 5.9 TRANSPORT PARAMETER PREDICTED VALUES MULTIPLE REGRESSION $\bar{\Phi}_b$
CHALMERS	1	0.00471	0.00466	0.00431	0.00000	0.00537	0.00527
	2	0.00574	0.00577	0.00541	0.00000	0.00742	0.00748
	3	0.00719	0.00731	0.00665	0.00000	0.00956	0.00978
	4	0.00929	0.00958	0.00868	0.01442	0.01249	0.01302
	5	0.01901	0.02003	0.01844	0.02234	0.02274	0.02430
	6	0.03278	0.03451	0.03301	0.01919	0.03303	0.03505
	7	0.00362	0.00322	0.00334	0.00000	0.00297	0.00250
	8	0.00925	0.00890	0.00873	0.00000	0.01125	0.01065
	9	0.01239	0.01230	0.01270	0.00744	0.01493	0.01476
	10	0.01172	0.01166	0.01133	0.00000	0.01422	0.01409
	11	0.01852	0.01900	0.01820	0.04465	0.02030	0.02095
	12	0.03099	0.03265	0.03161	0.04178	0.02874	0.03064
	13	0.12122	0.12883	0.12900	0.05510	0.06357	0.06729
	14	0.00840	0.00756	0.00893	0.00000	0.01017	0.00879
	15	0.01540	0.01464	0.01586	0.00000	0.01654	0.01536
	16	0.01950	0.01911	0.02147	0.02754	0.01988	0.01927
	17	0.02954	0.02990	0.03312	0.02834	0.02603	0.02629
	18	0.04973	0.05217	0.05664	0.03612	0.03559	0.03757
	19	0.12098	0.13171	0.14339	0.00000	0.05767	0.06335
	20	0.00312	0.00319	0.00534	0.00000	0.00183	0.00183
	21	0.00386	0.00396	0.00653	0.00000	0.00330	0.00335
	22	0.00499	0.00514	0.00868	0.00000	0.00548	0.00563
	23	0.00619	0.00638	0.01098	0.00000	0.00746	0.00767
	24	0.00798	0.00819	0.01333	0.00000	0.00962	0.00981
	25	0.01122	0.01140	0.01901	0.00000	0.01347	0.01353
	26	0.00411	0.00419	0.00723	0.01395	0.00378	0.00383
	27	0.00709	0.00734	0.01185	0.02197	0.00796	0.00823
	28	0.01222	0.01271	0.02095	0.01882	0.01371	0.01424
	29	0.01560	0.01618	0.02693	0.01684	0.01675	0.01729
	30	0.00528	0.00542	0.00577	0.00000	0.00395	0.00417
	31	0.01649	0.01629	0.01901	0.00000	0.02131	0.02147
	32	0.04326	0.04056	0.05266	0.00000	0.04333	0.04019
	33	0.07199	0.06341	0.08754	0.00000	0.05950	0.05011
	34	0.00475	0.00479	0.00538	0.00000	0.00319	0.00328
	35	0.00882	0.00863	0.01005	0.00000	0.01151	0.01146
	36	0.01432	0.01347	0.01629	0.01851	0.01970	0.01851
	37	0.00845	0.00876	0.00943	0.00000	0.00973	0.01052
	38	0.02669	0.02656	0.03149	0.04307	0.03029	0.03075
	39	0.07613	0.07201	0.09006	0.02366	0.05824	0.05432
	40	0.02617	0.02630	0.01735	0.03801	0.03713	0.03870
	41	0.05420	0.05127	0.03732	0.05156	0.06086	0.05774
	42	0.07208	0.06535	0.05202	0.05941	0.07344	0.06537
	43	0.05206	0.05495	0.03618	0.03867	0.05285	0.05881
	44	0.10042	0.10250	0.07296	0.06195	0.07829	0.08236
NEWCASTLE	1	0.00701	0.00714	0.00401	0.01534	0.00740	0.00765
	2	0.02348	0.02334	0.01425	0.02833	0.02901	0.02890
	3	0.05049	0.04708	0.03161	0.02951	0.05012	0.04519
	4	0.01908	0.01976	0.01173	0.03584	0.02292	0.02431
	5	0.03261	0.03172	0.02034	0.00000	0.03730	0.03593
	6	0.06234	0.06098	0.04022	0.06030	0.05416	0.05225
	7	0.04171	0.04351	0.02787	0.04775	0.03933	0.04187
	8	0.03394	0.03541	0.02210	0.04711	0.03415	0.03644
	9	0.00398	0.00402	0.00236	0.00000	0.00097	0.00096
	10	0.01845	0.01747	0.01167	0.03268	0.02589	0.02411
	11	0.01011	0.01013	0.00595	0.00000	0.01349	0.01364

CHALMERS TEKNISKA HÖGSKOLA
Institutionen för vattenbyggnad

Report Series A

A:1 Bergdahl, L.: Physics of ice and snow as affects thermal pressure. 1977.

A:2 Bergdahl, L.: Thermal ice pressure in lake ice covers. 1978.

A:3 Häggström, S.: Surface Discharge of Cooling Water. Effects of Distortion in Model Investigations. 1978.

A:4 Sellgren, A.: Slurry Transportation of Ores and Industrial Minerals in a Vertical Pipe by Centrifugal Pumps. 1978.

A:5 Arnell, V.: Description and Validation of the CTH-Urban Runoff Model. 1980.

A:6 Sjöberg, A.: Calculation of Unsteady Flows in Regulated Rivers and Storm Sewer Systems. 1976.

A:7 Svensson, T.: Water Exchange and Mixing in Fjords. Mathematical Models and Field Studies in the Byfjord. 1980.

A:8 Arnell, V.: Rainfall Data for the Design of Sewer Pipe Systems. 1982.

A:9 Lindahl, J., Sjöberg, A.: Dynamic Analysis of Mooring Cables. 1983.

A:10 Nilsdal, J-A.: Optimeringsmodellen ILSD. Beräkning av topografins inverkan på ett dagvattensystems kapacitet och anläggningskostnad. 1983.

A:11 Lindahl, J.: Implicit numerisk lösning av rörelseekvationerna för en förankringskabel. 1984.

A:12 Lindahl, J.: Modellförsök med en förankringskabel. 1985.

A:13 Lyngfelt, S.: On Urban Runoff Modelling. The Application of Numerical Models Based on the Kinematic Wave Theory. 1985.

A:14 Johansson, M.: Transient Motions of Large Floating Structures. 1986.

A:15 Mårtensson, N., Bergdahl, L.: On the Wave Climate of the Southern Baltic. 1987.

A:16 Moberg, G.: Wave Forces on a Vertical Slender Cylinder. 1988.

A:17 Perrusquía González, G.S.: Part-Full Flow in Pipes with a Sediment Bed. Part one: Bedform dimensions. Part two: Flow resistance. 1988.

A:18 Nilsdal, J-A.: Bedömning av översvämningsrisken i dagvattensystem. Kontrollberäkning med typregn. 1988.

A:19 Johansson, M.: Barrier-Type Breakwaters. Transmission, Reflection and Forces. 1989.

A:20 Rankka, W.: Estimating the Time to Fatigue Failure of Mooring Cables. 1989.

A:21 Olsson, G.: Hybridelementmetoden, en metod för beräkning av ett flytande föremåls rörelse. 1990.

A:22 Perrusquía González, G.S.: Bedload Transport in Storm Sewers. Stream Traction in Pipe Channels. 1991.

CHALMERS TEKNISKA HÖGSKOLA
Institutionen för vattenbyggnad

Report Series B

B:1 Bergdahl, L.: Beräkning av vågkrafter. (Ersatts med 1979:07) 1977.

B:2 Arnell, V.: Studier av amerikansk dagvattenteknik. 1977.

B:3 Sellgren, A.: Hydraulic Hoisting of Crushed Ores. A feasibility study and pilot--plant investigation on coarse iron ore transportation by centrifugal pumps. 1977.

B:4 Ringesten, B.: Energi ur havsströmmar. 1977.

B:5 Sjöberg, A., Asp, T.: Brukar-anvisning för ROUTE-S. En matematisk modell för beräkning av icke-stationära flöden i floder och kanaler vid strömmande tillstånd. 1977.

B:6 Annual Report 1976/77. 1977.

B:7 Bergdahl, L., Wernersson, L.: Calculated and Expected Thermal Ice Pressures in Five Swedish Lakes. 1977.

B:8 Göransson, C-G., Svensson, T.: Drogue Tracking - Measuring Principles and Data Handling. 1977.

B:9 Göransson, C-G.: Mathematical Model of Sewage Discharge into confined, stratified Basins - Especially Fjords. 1977.

B:10 Arnell, V., Lyngfelt, S.: Beräkning av dagvattenavrinning från urbana områden. 1978.

B:11 Arnell, V.: Analysis of Rainfall Data for Use in Design of Storm Sewer Systems. 1978.

B:12 Sjöberg, A.: On Models to be used in Sweden for Detailed Design and Analysis of Storm Drainage Systems. 1978.

B:13 Lyngfelt, S.: An Analysis of Parameters in a Kinematic Wave Model of Overland Flow in Urban Areas. 1978.

B:14 Sjöberg, A., Lundgren, J., Asp, T., Melin, H.: Manual för ILLUDAS (Version S2). Ett datorprogram för dimensionering och analys av dagvattensystem. 1979.

B:15 Annual Report 1978/79. 1979.

B:16 Nilsdal, J-A., Sjöberg, A.: Dimensionerande regn vid höga vattenstånd i Göta älv. 1979.

B:17 Stöllman, L-E.: Närkes Svartå. Hydrologisk inventering. 1979.

B:18 Svensson, T.: Tracer Measurements of Mixing in the Deep Water of a Small, Stratified Sill Fjord. 1979.

B:19 Svensson, T., Degerman, E., Jansson, B.,Westerlund, S.: Energiutvinning ur sjö- och havssediment. En förstudie. R76:1980. 1979.

B:20 Annual Report 1979. 1980.

B:21 Stöllman, L-E.: Närkes Svartå. Inventering av vattentillgång och vattenanvändning. 1980.

Report Series B

B:22 Häggström, S., Sjöberg, A.: Effects of Distortion in Physical Models of Cooling Water Discharge. 1979.

B:23 Sellgren, A.: A Model for Calculating the Pumping Cost of Industrial Slurries. 1981.

B:24 Lindahl, J.: Rörelseekvationen för en kabel. 1981.

B:25 Bergdahl, L., Olsson, G.: Konstruktioner i havet. Vågkrafter-rörelser. En inventering av datorprogram. 1981.

B:26 Annual Report 1980. 1981.

B:27 Nilsdal, J-A.: Teknisk-ekonomisk dimensionering av avloppsledningar. En litteraturstudie om datormodeller. 1981.

B:28 Sjöberg, A.: The Sewer Network Models DAGVL-A and DAGVL-DIFF. 1981.

B:29 Moberg, G.: Anläggningar för oljeutvinning till havs. Konstruktionstyper, dimensioneringskriterier och positioneringssystem. 1981.

B:30 Sjöberg, A., Bergdahl, L.: Förankringar och förankringskrafter. 1981.

B:31 Häggström, S., Melin, H.: Användning av simuleringsmodellen MITSIM vid vattenresursplanering för Svartån. 1982.

B:32 Bydén, S., Nielsen, B.: Närkes Svartå. Vattenöversikt för Laxå kommun. 1982.

B:33 Sjöberg, A.: On the stability of gradually varied flow in sewers. 1982.

B:34 Bydén, S., Nyberg, E.: Närkes Svartå. Undersökning av grundvattenkvalitet i Laxå kommun. 1982.

B:35 Sjöberg, A., Mårtensson, N.: Regnenveloppmetoden. En analys av metodens tillämplighet för dimensionering av ett 2-års perkolationsmagasin. 1982.

B:36 Svensson, T., Sörman, L-O.: Värmeupptagning med bottenförlagda kylslangar i stillastående vatten. Laboratorieförsök. 1982.

B:37 Mattsson, A.: Koltransporter och kolhantering. Lagring i terminaler och hos storförbrukare. (Delrapport). 1983.

B:38 Strandner, H.: Ett datorprogram för sammankoppling av ILLUDAS och DAGVL-DIFF. 1983.

B:39 Svensson, T., Sörman, L-O.: Värmeupptagning med bottenförlagda slangar i rinnande vatten. Laboratorieförsök. 1983.

B:40 Mattsson, A.: Koltransporter och kolhantering. Lagring i terminaler och hos storförbrukare. Kostnader. Delrapport 2. 1983.

B:41 Häggström, S., Melin, H.: Närkes Svartå. Simuleringsmodellen MITSIM för kvantitativ analys i vattenresursplanering. 1983.

B:42 Hård, S.: Seminarium om miljöeffekter vid naturvärmesystem. Dokumentation sammanställd av S. Hård, VIAK AB. BFR-R60:1984. 1983.

B:43 Lindahl, J.: Manual för MODEX-MODIM. Ett datorprogram för simulering av dynamiska förlopp i förankringskablar. 1983.

Report Series B

B:44 Activity Report. 1984.

B:45 Sjöberg, A.: DAGVL-DIFF. Beräkning av icke-stationära flödesförlopp i helt eller delvis fyllda avloppssystem, tunnlar och kanaler. 1984.

B:46 Bergdahl, L., Melin, H.: WAVE FIELD. Manual till ett program för beräkning av ytvattenvågor. 1985.

B:47 Lyngfelt, S.: Manual för dagvattenmodellen CURE. 1985.

B:48 Perrusquía, G., Lyngfelt, S., Sjöberg, A.: Flödeskapacitet hos avloppsledningar delvis fyllda med sediment. En inledande experimentell och teoretisk studie. 1986.

B:49 Lindahl, J., Bergdahl, L.: MODEX-MODIM. User's Manual. 1987.

B:50 Mårtensson, N.: Dynamic Analysis of a Moored Wave Energy Buoy. 1988.

B:51 Lyngfelt, S.: Styrning av flöden i avloppssystem. Begrepp - Funktion - FoU-Behov. 1989.

B:52 Perrusquía, G.: Sediment in Sewers. Research Leaves in England. 1990.

B:53 Lyngfelt, S.: Simulering av ytavrinning i dagvattensystem. 1991.